

ION EXCHANGE EQUILIBRIUM: SELECTIVITY COEFFICIENT AND ION  
EXCHANGE CAPACITY, HEAVY METALS REMOVAL, AND MATHEMATICAL  
MODELLING

ION EXCHANGE EQUILIBRIUM: SELECTIVITY COEFFICIENT AND ION  
EXCHANGE CAPACITY, HEAVY METALS REMOVAL, AND MATHEMATICAL  
MODELLING

By: MARYANNE CALUORI, B.Sc.

A Thesis Submitted to the School of Graduate Studies in Partial Fulfillment of the  
Requirements for the Degree Master of Applied Science

McMaster University © Copyright by Maryanne Caluori, July 2020

McMaster University MASTER OF APPLIED SCIENCE (2020) Hamilton, Ontario  
(Civil Engineering)

TITLE: Ion exchange equilibrium: selectivity coefficient and ion exchange capacity,  
heavy metals removal, and mathematical modelling

AUTHOR: Maryanne Caluori, B.Sc. (McMaster University)

SUPERVISOR: Dr. Younggy Kim

NUMBER OF PAGES: iii, 52

## Abstract

This research conducted equilibrium experiments to determine ion exchange equilibria data for the inorganic cations  $\text{Ca}^{2+}$ ,  $\text{Na}^+$ , and  $\text{NH}_4^+$  for binary cation exchange involving sulfonic acid, polystyrene gel resins saturated with  $\text{Na}^+$  or  $\text{NH}_4^+$ . A linear least-square fitting was developed to find representative ion exchange capacity (IEC) and selectivity coefficient (K) values. Equilibrium experiments were utilized to test the developed new linearization method for binary systems: Ca- $\text{NH}_4$ ; Ca- $\text{Na}$ ; and  $\text{Na}$ - $\text{NH}_4$  using three commercial strong acid cation (SAC) exchange resins. It was determined that SAC exchange resins saturated with  $\text{NH}_4^+$  were more selective towards  $\text{Ca}^{2+}$  than resins saturated with  $\text{Na}^+$ . The valency and the size of the hydrated radius of the counterion influenced the selectivity of binary systems. A higher valence and a smaller hydrated radius resulted in an increased affinity of the resin for ions. Results can be used to estimate the technical and economic feasibility of a design process along with the estimation of the effect of a change in operating conditions. In addition, the removal of toxic heavy metals was also investigated with an initial metal concentration of 0.1 mg/L. Results showed that the maximum percent removal of toxic heavy metal ions,  $\text{Cr}^{3+}$ ,  $\text{Pb}^{2+}$ ,  $\text{Ba}^{2+}$ , and  $\text{Cd}^{2+}$  ranged from ~ 95-99% when present in a solution containing a high molar concentration of  $\text{Ca}^{2+}$ ,  $\text{Na}^+$ , and  $\text{NH}_4^+$ . It was observed that SAC exchange resins can effectively remove toxic heavy metals at very low concentrations. The high selectivity that SAC exchange resins possess towards heavy metals proves that they can be used as a pretreatment method for the removal of toxic heavy metals from municipal and industrial wastewaters. Moreover, the performance of SAC exchange resins for the removal of  $\text{Ca}^{2+}$  from waste solutions was

investigated through computer modelling. Results showed that ion exchange is an efficient method for the removal of  $\text{Ca}^{2+}$ . A sensitivity analysis showed that the variation in K and IEC greatly influenced the breakthrough time as an increase in both parameters resulted in greater  $\text{Ca}^{2+}$  uptake. Modelling results can be used to optimize the design of ion exchange systems for the pretreatment of inorganic cations which can reduce membrane scaling.

## **Acknowledgments**

I would like to thank my family and boyfriend for their encouragement and unconditional support throughout these two years.

I would like to sincerely thank my supervisor, Dr. Younggy Kim for his guidance and insight. I am very grateful for the opportunity to grow and learn under your support and supervision. It was a privilege to be mentored by such a knowledgeable researcher. Thank you to Dr. Zhao and Dr. de Lannoy for their time and expertise as members of my examination committee. I would also like to thank Monica Han for her assistance and expertise in the lab. Finally, I would like to thank all my lab mates and friends in JHE 330 for all their guidance and company throughout the last two years.

This study was conducted with collaboration of Suez Water Technologies and Solutions as well as with the research supports from Ontario Ministry of Research, Innovation and Science (Early Researcher Awards and Ontario Research Fund-Research Excellence).

## Table of Contents

Abstract .....	iii
Acknowledgments.....	v
Table of Contents .....	vi
List of Tables .....	vii
List of Figures .....	ix
Abbreviations and Symbols .....	x
1. Introduction.....	1
1.1. Literature Review: ion exchange resins .....	3
1.1.1 Ion exchange process .....	3
1.1.2 Ion exchange materials and properties .....	4
1.1.3 Ion exchange resin applications .....	10
1.2 Literature Review: determination of ion exchange capacity and selectivity coefficient	10
1.3 Literature Review: heavy metal removal using SAC exchange resins .....	14
1.4 Literature Review: ion exchange column .....	16
2. Methodology .....	18
2.1. Experimental .....	18
2.1.1. Cation exchange resins.....	18
2.1.2. Equilibrium experiments.....	20
2.1.3. Analytical methods .....	22
2.2. Determination of ion exchange capacity and selectivity coefficient.....	22
2.2.1. Linearization Method #1 .....	23
2.2.2. Linearization Method #2.....	24
2.3. Ion exchange column model development.....	25
3. Results and Discussion.....	27
3.1. Determination of IEC and $K_{Ca/NH_4}$ by linearization Method #1 .....	27
3.2. Determination of IEC and $K_{Ca/NH_4}$ by linearization Method #2 .....	28
3.3. Propagation of small analytical errors in the two linearization methods .....	29
3.4. Determination of IEC and $K_{Ca/Na}$ by linearization Method #2 .....	31
3.5. Selectivity of divalent over monovalent cations .....	33
3.6. Competition between $Na^+$ and $NH_4^+$ .....	34

3.7.	Heavy metal removal .....	36
3.8.	One-dimensional column model .....	39
3.8.1.	Concentration time profile of $\text{Ca}^{2+}$ and $\text{NH}_4^+$ .....	39
3.8.2.	Effect of $K_{\text{Ca}/\text{NH}_4}$ , IEC, porosity, and velocity on calcium removal .....	41
4.	Conclusions .....	43
4.1.	Determination of IEC and $K_{\text{Ca}/\text{NH}_4}$ , $K_{\text{Ca}/\text{Na}}$ , $K_{\text{Na}/\text{NH}_4}$ by linearization .....	43
4.2.	Heavy metal removal .....	44
4.3.	One-dimensional column model .....	45
4.4.	Future Work .....	45
4.4.1.	Determination of IEC and K of multicomponent systems .....	45
4.4.2.	One-dimensional column model .....	46
	References .....	47



## List of Tables

Table 1.1: Characterization of ion exchange resins .....	5
Table 1.2: Hydrated radius of cations .....	9
Table 2.1. Strong cation exchange resin properties .....	19
Table 2.2: Average wastewater characteristics of Woodward dewatering centrate. (n=3) .....	20
Table 2.3: Experimental conditions used for different binary systems studied .....	20
Table 2.4: Initial model parameters for a one-dimensional ion exchange column. ....	27
Table 3.1: Effect of variation in Methods 1 and 2 on (A) IEC (eq/L); (B) $K_{CaNH_4}$ (kg/L) for Resins A, B, C. ....	30
Table 3.2: Heavy metal concentration limits found in municipal wastewater effluent.....	38

## List of Figures

Figure 1.1. Structure of cation exchange resin.....	5
Figure 2.1: Schematic diagram for the mass balance of a solute in a segment of a column. ....	26
Figure 3.1: Determination of IEC and K for Ca-NH <sub>4</sub> system: (A) Resin A; (B) Resin B; (C) Resin C.....	28
Figure 3.2: Determination of IEC and K for Ca-NH <sub>4</sub> system: (A) Resin A; (B) Resin B; (C) Resin C.....	29
Figure 3.3: Determination of IEC and K for Ca-Na system: (A) Resin A; (B) Resin B; (C) Resin C.....	32
Figure 3.4: Determination of K for Na- NH <sub>4</sub> system: (A) Resin A; (B) Resin B; (C) Resin C. ....	35
Figure 3.5: Percent removal of heavy metals from various binary systems. (n = 2; results based on the average and standard deviation).....	38
Figure 3.6: Concentration time profile of Ca <sup>2+</sup> and NH <sub>4</sub> <sup>+</sup> . ....	40
Figure 3.7: Effect of variation in model parameter values on breakthrough profile: (A) selectivity coefficient (K <sub>Ca/NH<sub>4</sub></sub> ); (B) ion exchange capacity (IEC); (C) porosity (ε); (D) flow velocity (V)...	42

## Abbreviations and Symbols

### Abbreviations

DI	Deionized water
DVB	Divinylbenzene
MTZ	Mass Transfer Zone
SAC	Strong Acid Cation Exchange Resin
SBA	Strong Base Anion Exchange Resin
WAC	Weak Acid Cation Exchange Resin
WBA	Weak Base Anion Exchange Resin

### Symbols

		<i>Unit</i>
$a_i$	aqueous phase activity of species $i$	[ - ]
$\bar{a}_i$	resin phase activity of species $i$	[ - ]
Å	ångström	[ - ]
$A$	cross sectional area	[cm <sup>2</sup> ]
$A$	divalent cation in aqueous or resin phase	[ - ]
$B$	monovalent cation in aqueous or resin phase	[ - ]
$c_i$	equilibrium aqueous phase concentration of species $i$	[mM], [meq/mL]
$\frac{dc}{dt}$	rate of ion exchange in aqueous phase	[mM]
$\frac{dq}{dt}$	rate of ion exchange in resin phase	[mmol/g]
IEC	ion exchange capacity	[mmol/g], [eq/L]
$K$	selectivity coefficient, generalized	[ - ]
$K_{A/B}$	selectivity coefficient of divalent to monovalent cation	[g/L], [kg/L]
$K_{B/B}$	selectivity coefficient of monovalent to monovalent cation	[ - ]
$m$	mass of resin	[g]
$pK$	acid/base dissociation constant	[ - ]

$q_i$	equilibrium resin phase concentration of species $i$	[mmol/g]
$Q$	volumetric flow rate	[cm <sup>3</sup> / min]
$\overline{R^-}$	active site on the resin backbone	[ - ]
$\Delta t$	time	[min]
$v$	volume	[L], [cm <sup>3</sup> ]
$V$	flow velocity	[cm/min]
$\bar{X}$	average	[ - ]
$\Delta Z, dz$	column grid thickness	[cm]
$Z$	height of column	[cm]
$z$	ionic charge	[ - ]
$\varepsilon$	porosity	[ - ]
$\rho$	resin density	[ g/L ]
$\sigma$	standard deviation	[ - ]

***Subscripts***

A	species A, divalent cation	[ - ]
B	species B, monovalent cation	[ - ]
A + B	sum of ionic concentrations of species A and B	[ - ]
0	initial concentration	[ - ]
e	equilibrium concentration	[ - ]
in	inlet	[ - ]
out	outlet	[ - ]

***Superscripts***

$t, t + 1$	time step	[ - ]
$n, n - 1$	column grid number	[ - ]
$z$	valence charge of species $i$	[ - ]

## 1. Introduction

Ion exchange is a widely employed technology in food and beverage industry, hydrometallurgy, metals finishing, chemical, petrochemical, pharmaceutical technology, sugar and sweetener production, ground and potable water treatment, nuclear, softening, industrial water treatment, semiconductor, power, and many other industries (Crittenden et al., 2012; Bochenek et al., 2011; Helfferich, 1962; Spiro, 2009). In ion exchange, a reversible interchange of ions between the solid and aqueous phases occurs as an insoluble substance (resin) removes ions from an electrolytic solution and releases ions of the same charge in a chemically equivalent amount (Crittenden et al., 2012; Oancea et al., 2008). In a separation process with ion exchange resins, the process efficiency is substantially influenced by (1) the resins preference for ions of a higher charge, (2) ions of smaller hydrated radius are preferred, and (3) ions which interact strongly with the functional groups of the resin (Alyüz & Veli, 2009; Crittenden et al., 2012). Much effort has been focused on characterizing the chemical and physical properties of resins to predict their usefulness (Helfferich, 1962). The characterization of ion exchange capacity (IEC) and selectivity coefficient (K) provides information on the preference in which the resin has for contaminants, therefore, it will be useful when designing ion exchange systems to remove multiple contaminants (Crittenden et al., 2012; Foster et al., 2016).

Among the materials used in ion exchange processes, strong acid cation (SAC) exchange resins are employed and used in the separation of toxic heavy metals and inorganic cations from aqueous solutions (Bochenek et al., 2011; Prajapati, 2014; Spiro, 2009). Heavy metals are one of the most persistent pollutants in wastewater. The discharge

of high amounts of heavy metals into water bodies leads to several environmental and health impacts (Akpor et al., 2014). The most common heavy metals in wastewater include  $\text{Ag}^+$ ,  $\text{As}^{3-}$ ,  $\text{Ba}^{2+}$ ,  $\text{Cd}^{2+}$ ,  $\text{Cr}^{3+}$ ,  $\text{Hg}^{2+}$ ,  $\text{Pb}^{2+}$ , and  $\text{Se}^{2-}$  (Akpor et al., 2014). These heavy metal ions are found in various wastewaters and are included on the list of Toxic Substances of the Canadian Environmental Protection Act, CEPA 1999 (ECCC, 2012). Classical techniques of heavy metal removal include the following processes: precipitation, flocculation, ion exchange, and adsorption (Alyüz & Veli, 2009; Yu et al., 2009). Among these processes, the most common are ion exchange and chemical precipitation (Abo-Farha et al., 2009; Kurniawan et al., 2006). The main advantages of ion exchange over other techniques are the recovery of metal value, high selectivity, less sludge volume produced, and the ability to meet strict discharge specifications (Abo-Farha et al., 2009; Alyüz & Veli, 2009; Kurniawan et al., 2006).

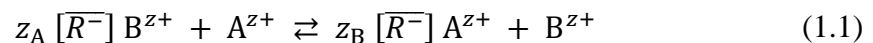
In addition, SAC exchange resins are considered a viable technology for the removal of inorganic cations. The common methods for inorganic cation removal from aqueous solutions can be ordered as chemical precipitation, ion exchange, ultrafiltration, reverse osmosis, electrodialysis, and adsorption (Yu et al., 2009). In water and wastewater treatment a common problem faced is the mineralization of inorganic solids on the surface of the membrane, known as membrane scaling (Brewster et al., 2017). To address this issue, feed pretreatment using filtration, coagulation, and flocculation or acid cleaning are performed (Brewster et al., 2017; Mondor et al., 2009). Each of these processes requires additional cost and operational downtime (Brewster et al., 2017; Greenlee et al., 2009).

The goal of this research is (1) to develop a linear system for plotting experimental data leading to the determination of IEC and K. The characterization of both parameters will provide information on the preference in which SAC exchange resins have towards inorganic cations,  $\text{Na}^+$ ,  $\text{NH}_4^+$ , and  $\text{Ca}^{2+}$ . This paper will report the ion exchange equilibria data for Ca- $\text{NH}_4$ ; Ca-Na; and Na- $\text{NH}_4$  systems. Two other research objectives are: (2) to determine the ability of SAC exchange resins to effectively remove toxic heavy metals from a solution containing a relatively low molar concentration of heavy metals and a high molar concentration of  $\text{Na}^+$ ,  $\text{NH}_4^+$ , and  $\text{Ca}^{2+}$ ; and (3) to simulate a one-dimensional ion exchange column reactor as a pretreatment process for the removal of divalent cations (e.g.,  $\text{Ca}^{2+}$ ) which can cause serious inorganic scaling problems in membrane separation processes.

## **1.1. Literature Review: ion exchange resins**

### **1.1.1 Ion exchange process**

Ion exchangers are insoluble solid materials that carry exchangeable cations or anions (Zagorodni, 2007). When the ion exchanger is in contact with an electrolyte solution, these ions are exchanged with an equivalent number of other ions of the same charge (Zagorodni, 2007). An internal osmotic pressure is established through the interchanging of ions between the ion exchanger and solution (Crittenden et al., 2012). The cation exchange reaction can be represented by the following equation:



where  $\overline{R}^-$  represents the ionic group attached to the ion exchange resin and A and B are the exchanging ions.  $z_A$  and  $z_B$  represent the valency of the exchanging ion and the superscript  $z$  is the valency of species A or B. Ion exchange is a stoichiometric process, therefore, ion exchange media will continue exchanging ions until equilibrium has been achieved. This is to satisfy the principle of electroneutrality (Crittenden et al., 2012).

### **1.1.2 Ion exchange materials and properties**

Within literature, there are several different natural and synthetic materials that show ion exchanging properties. The predominant type of exchanger used today is synthetic resins due to their characteristics that can be tailored to specific applications. Ion exchange resins are composed of a three-dimensional, crosslinked polymer matrix containing covalently bonded functional groups with fixed ionic charges (Crittenden et al., 2012; Zagorodni, 2007). The backbone of the resin consists of vinyl polymers (polystyrene and polyacrylic) and divinylbenzene (DVB) which is used to crosslink the polymer to the resin backbone (Crittenden et al., 2012; Zagorodni, 2007). The structure of a cation exchange resin is illustrated in Figure 1.1. Crosslinking provides the fundamental chemical bonding between adjacent polymer chains, therefore, giving the resin its inherent physical strength (Harland, 1994). As crosslinking increases the following characteristics are observed, (1) the resin bead becomes stronger, (2) more active sites are introduced (higher capacity), and (3) the resin structure is tighter (reduction in moisture content) (Crittenden et al., 2012).



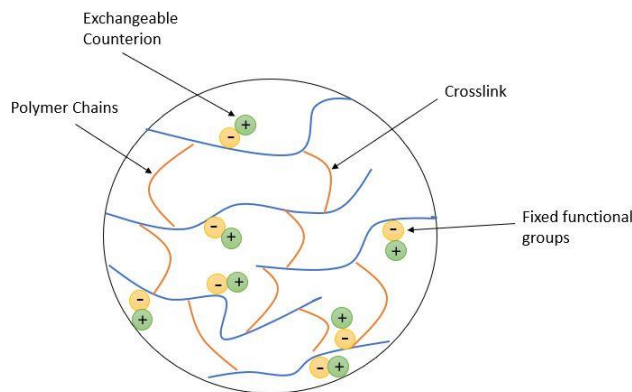


Figure 1.1. Structure of cation exchange resin

The nature of an ion exchange resin is determined by the functional groups attached to the resin matrix (Crittenden et al., 2012; Zagorodni, 2007). Based on the functional groups bonded to the resin backbone, ion exchange resins can be classified into four categories based on Table 1.1 (Crittenden et al., 2012). The distinctions are based on  $pK$  values of the functional groups (Crittenden et al., 2012).

Table 1.1: Characterization of ion exchange resins

Resin Type	Functional Group	$pK$	Ion Exchange Capacity (eq/L)
Strong acid cation (SAC)	Sulfonate ( $SO_3^-$ )	$< 0$	1.7-2.1
Weak acid cation (WAC)	Carboxylate ( $COO^-$ )	4-5	4-4.5
Strong base anion (SBA)	Quaternary amine ( $N^+(CH_3)_3$ )	$> 13$	1-2.5
Weak base anion (WBA)	Tertiary amine ( $N^+(CH_3)_2$ )	5.7-7.3	2-3

Ion exchange resins contain a wide variety of properties that make them ideal for water and wastewater treatment applications. Such properties can be divided into chemical and physical properties. Ion exchange capacity (IEC) and selectivity coefficient ( $K$ ), are

two important chemical parameters used in considering column design and operation. Moreover, resin swelling and regeneration are two important physical properties. These properties are important in the selection of resins for specific water treatment applications.

IEC is defined as the number of functional groups within the ion exchange resin (Crittenden et al., 2012; Zagorodni, 2007). IEC is an important property as it determines the number of counterions that can be exchanged onto the resin (Crittenden et al., 2012). IEC is dependant upon the moisture content of the resin, therefore, given two different ionic forms of the same resin, IEC will differ due to the differences in water content attributed to resin swelling (Crittenden et al., 2012). Given that sites in the ion exchange resin are assumed to always be occupied by species A or B, the following IEC equation can be written as:

$$\text{IEC} = q_A + q_B \quad (1.2)$$

where  $q_A, q_B$  represent equilibrium resin phase concentrations.

K is another important chemical parameter within ion exchange and is defined as the affinity or preference of the resin for one ion in comparison with another ion in the aqueous phase (Crittenden et al., 2012; Zagorodni, 2007). The selectivity equation for species A over species B can be written as follows:

$$K_{A/B} = \frac{[q_{A^\pm}]^{z_B} \cdot [c_{B^\pm}]^{z_A}}{[c_{A^\pm}]^{z_B} \cdot [q_{B^\pm}]^{z_A}} \quad (1.3)$$

where  $K_{A/B}$  is the selectivity coefficient for the exchange of species B with species A onto the resin,  $c_A, c_B$  and  $q_A, q_B$  represent the aqueous and resin phase concentrations and  $z$  is the valence number of the exchanging ion (Crittenden et al., 2012; Zagorodni, 2007). Any

units can be chosen for aqueous and resin phase concentrations; however, they must remain constant (Benjamin & Lawler, 2013). Units for  $K_{A/B}$  come from the chosen units of both aqueous and resin phase concentrations (Benjamin & Lawler, 2013). According to Equation (1.3), the preference for species A over species B leads to the numerical value of  $K_{A/B} > 1$ . If species B is more preferred by the resin, the value will be  $< 1$ .

The affinity of the resin for one ion over another is influenced by (1) the valency of the counterion, (2) the diameter of the counterions hydrated radius, and (3) the concentration of the counterion in an aqueous solution (Crittenden et al., 2012). For dilute aqueous phase concentrations at temperatures encountered in water and wastewater treatment, ion exchange resins prefer counterions of a higher valency (Crittenden et al., 2012). For SAC exchange resins, the preference is as follows:  $Fe^{3+} > Al^{3+} > Ba^{2+} > Pb^{2+} > Sr^{2+} > Ca^{2+} > Ni^{2+} > Cd^{2+} > Cu^{2+} > Co^{2+} > Zn^{2+} > Mg^{2+} > Ag^+ > Cs^+ > Rb^+ > K^+ > NH_4^+ > Na^+ > H^+$  (Hubicki & Kołodyńska, 2012; Sahu & Jaiswani, 2018). In the preference shown above, it is assumed that the spacing of the functional groups allows for the exchange of multivalent ions (Crittenden et al., 2012). The above preference is observed as counterions with a higher valency are preferred by the resin as it results in reduced resin swelling (Crittenden et al., 2012). As a resin encounters counterions in the aqueous phase, large concentration gradients exist between the ions in the aqueous phase and the resin phase (Crittenden et al., 2012). The tendency is for aqueous ions to migrate into the resin phase and ions in the resin phase to migrate into the aqueous phase (Crittenden et al., 2012). The initial migration of ions establishes the Donnan potential (Crittenden et al., 2012). The potential attracts aqueous phase ions into the resin to balance the diffusion of the resin

phase ions entering the aqueous phase solution (Crittenden et al., 2012). When equilibrium is achieved, the potential approaches zero (Crittenden et al., 2012). The force exerted by the Donnan potential on an ion is proportional to the valence of the ion (Helfferich 1962; Crittenden et al., 2012). The Donnan potential increases as the aqueous phase concentrations become more dilute (Crittenden et al., 2012). For solutions with large aqueous phase concentrations, the exchange potentials of ions of different valences become negligible and ions of lower valence can sometimes be more preferred (Crittenden et al., 2012; Zagorodni, 2007).

Resin selectivity can also be influenced by the degree of swelling or pressure within the resin bead (Crittenden et al., 2012; Zagorodni, 2007). In solution, both aqueous and resin phase ions have water molecules that surround them (Crittenden et al., 2012; Zagorodni, 2007). The group of water molecules surrounding each ion is called the radius of hydration (Crittenden et al., 2012; Zagorodni, 2007). When ions diffuse in solution, the water molecules associated with these ions move as well (Crittenden et al., 2012). The crosslinking bonds that hold the resin matrix together oppose the osmotic forces exerted by these exchanged ions (Crittenden et al., 2012). These opposing forces cause the swelling pressure (Crittenden et al., 2012). In a dilute aqueous solution, ion exchange resins prefer counterions with a smaller hydrated radius as they reduce the swelling pressure of the resin and are more tightly bound to the resin (Crittenden et al., 2012; Zagorodni, 2007). Table 1.2 outlines the hydrated radii of various cations used in this study. For solutions with large aqueous phase concentrations, the rule that the smallest hydrated ion shows the greatest

exchange potential may not hold true. This can result in ions with a larger hydrated radius to be more preferred by the resin (Crittenden et al., 2012; Zagorodni, 2007).

Table 1.2: Hydrated radius of cations

Ion	Hydrated Radius (Å) <sup>a</sup>
Na <sup>+</sup>	3.58
NH <sub>4</sub> <sup>+</sup>	3.31
Ca <sup>2+</sup>	4.12

<sup>a</sup> The hydrated radius was obtained from Nightingale et al., 1959

The ability of resin to swell is one of the most important physical properties of ion exchange resins. The amount of moisture retained by resin is determined by the crosslinking and type of functional group attached to the resin matrix (Crittenden et al., 2012). For all resin types, the percentage of swelling decreases as the degree of crosslinking increases (Crittenden et al., 2012). This is due to a highly crosslinked resin ( $\geq 16\%$ ) being more rigid, therefore, resulting in a reduced ability to swell in comparison to lower crosslinked resins (Zagorodni, 2007). In addition, the nature of the counterion plays a role in the degree of swelling. A decrease in swelling is observed in counterions with a higher valence and a smaller hydrated radius (Crittenden et al., 2012; Zagorodni, 2007).

Ion exchange resins also can regenerate once equilibrium has been achieved. This process involves the circulation of a regenerant solution to remove all previously exchanged ions from the resin (Crittenden et al., 2012; Zagorodni, 2007). The ability of resins to be regenerated is advantageous as it allows for many years of usage which is cost effective (Spiro, 2009).

### **1.1.3 Ion exchange resin applications**

Ion exchange is a well developed and effective method present in numerous industrial applications. The process of ion exchange is considered attractive due to the relative simplicity in application and operation (Bochenek et al., 2011; Spiro, 2009). In many cases, ion exchange has proven to be economic and sustainable as their insolubility provides cycles of loading, regeneration and reloading, allowing for many years of usage (Spiro, 2009). Ion exchange resins are most used in the treatment of drinking and wastewater in commercial and industrial applications such as water softening, dealkalisation and demineralization (Bochenek et al., 2011; Prajapati, 2014; Spiro, 2009). Additional applications include the removal of toxic heavy metals, wastewater decontamination, radioactive waste treatment, hydrometallurgy, biomolecular separations, and chemical processing (Prajapati, 2014; Spiro, 2009; Wheaton and Lefevre, 2000).

### **1.2 Literature Review: determination of ion exchange capacity and selectivity coefficient**

The characterization of a resin and the prediction of exchange equilibria, IEC and K, have been the subject of investigation since the late 1940s (Boyer et al., 1999). Much effort has been focused on characterizing the chemical and physical properties of resins to predict their usefulness (Helfferich, 1962). The characterization of both IEC and K is advantageous as it allows for determining the number of ionic constituents retained by the resin and provides information on which ionic constituents are preferred (Crittenden et al., 2012). From the determination of both parameters, relationships can be used to estimate

technical and economic feasibility of a design process along with the estimation in the effect of a change in operating conditions (Boyer et al., 1999; Crittenden et al., 2012; Klein et al., 1967).

In determining IEC and K of binary systems, primary emphasis has been placed on methods utilizing models based on mass action law and adsorption isotherms (Dranoff and Lapidus, 1957). Since the pioneering work of Donnan (1924), the determination of equilibrium between an ion exchanger and an aqueous solution has been a subject of debate (Donnan 1924; Fievet, 2015; Manning & Melshelmer, 1983). Donnan (1924) introduced the theory of Donnan equilibrium referring to the distribution of ions between two phases separated by a semipermeable boundary. Following the work of Donnan (1924), Gaines and Thomas (1953) developed a model predicting the characteristics of ion exchange equilibria using thermodynamic principles (Boyer, 1995; Gaines & Thomas, 1953). Additional developments by Boyd et al. (1947), Crank and Park (1968), Kressman and Kitchener (1949) led to the introduction of separation factors, however, they did not reflect the effect of ionic valence. Due to the limitation, this method led to strong composition dependences when both ions are not of the same valence (Manning & Melsheimer, 1983). Much of the work in the determination of equilibria have used some derivative of Donnan equilibrium which can be written using the equation based on mass law:

$$K_{A/B} = \frac{\bar{a}_A^{z_B} \cdot a_B^{z_A}}{\bar{a}_B^{z_A} \cdot a_A^{z_B}} \quad (1.4)$$

where  $a_A$ ,  $a_B$  and  $\bar{a}_A$ ,  $\bar{a}_B$  are activities of ions A and B in the aqueous and resin phase and superscripts  $z_A$ ,  $z_B$  is the valence number of species A and B.  $K_{A/B}$  from Equation (1.4)

represents a thermodynamic equilibrium constant (Helfferich, 1962; Kressman and Kitchener, 1949).

The developed thermodynamic constant by previous authors is infrequently used in practice due to the difficulties faced in determining the ionic activities within the resin phase (Manning & Melsheimer, 1983). Therefore, Equation (1.5) was developed replacing activities with concentrations leading to the definition of the selectivity coefficient (Bauman and Eichhorn, 1947, Manning & Melsheimer, 1983; Soldano et al., 1995; Tombalakian et al., 1967).

$$K_{A/B} = \frac{q_A^{z_B} \cdot c_B^{z_A}}{q_B^{z_A} \cdot c_A^{z_B}} \quad (1.5)$$

where  $c_A, c_B$  and  $q_A, q_B$  are aqueous and resin phase concentrations of species A and B expressed in molality or equivalent per volume of solution and molality or equivalent per unit weight of resin, respectively. It is to be assumed that the activities are directly proportional to the equivalent concentrations of ions in both the aqueous and resin phase (Nachod, 1949).

Moreover, additional models were developed in determining equilibria parameters in terms of adsorption processes (Dranoff and Lapidus, 1957). Boyd et al. (1947) developed equations corresponding to the Langmuir adsorption isotherm. Following the work of Boyd et al. (1947), Bieber's (1954), studies developed various adsorption models, leading to a general adsorption equation resulting in the following:

$$\frac{c_A}{c_{0,A+B}} = \frac{q_A/IEC}{K_{A/B} - (K_{A/B} - 1) q_A/IEC} \quad (1.6)$$



where  $c_A$  (meq/ml) is the aqueous phase concentration,  $c_{0,A+B}$  (meq/ml) are the total ionic concentration of the aqueous solution and IEC (meq/g) and  $q$  (meq/g) are the ionic capacity and resin phase concentrations, respectively.

The majority of model development prior to the late 1950s focused on binary systems, containing only two competing ionic species (Boyer, 1995). Many scientists utilized model developments of binary systems to begin to characterize multicomponent systems. Estimation of equilibrium constants has been discussed by many authors, such as Dranoff and Lapidus (1957), Pieroni and Dranoff (1963), Smith and Woodburn (1978), Vasquez et al. (1986), Shallcross et al. (1988) and Mehablia et al. (1994). However, for this study, the focus will be placed on the determination of IEC and K from binary systems.

Limitations have resulted in the determination of IEC and K using various models. All models presented previously share the same limitation in that IEC must be determined in an experiment separate from equilibrium experiments used to determine K (Boyer, 1995). In addition, the result of the model modifications proposed by various methods has been to increase accuracy in determining both IEC and K experimentally (Boyer, 1995). However, this has led to an increase in the complexities of the models (Boyer, 1995). Therefore, the development of a simple yet accurate model for the determination of ion exchange equilibria from binary systems will be examined in this study.

### **1.3. Literature Review: heavy metal removal using SAC exchange resins**

Heavy metals are one of the most toxic persistent pollutants found in domestic and industrial wastewaters (Akpor et al., 2014; Tytła, 2019). Many heavy metals such as  $\text{Ag}^+$ ,  $\text{As}^{3-}$ ,  $\text{Ba}^{2+}$ ,  $\text{Cd}^{2+}$ ,  $\text{Cr}^{3+}$ ,  $\text{Hg}^{2+}$ ,  $\text{Pb}^{2+}$ , and  $\text{Se}^{2-}$  are water-soluble and non-biodegradable, leading to the adsorption into soils, plants, and living organisms, therefore, creating environmental, aquatic, and health impacts (Akpor et al., 2014; Kurniawan et al., 2006; Saidi, 2010). The heavy metals listed above are found in various wastewaters and are included on the list of Toxic Substances of the Canadian Environmental Protection Act, CEPA 1999 (ECCC, 2012). Various industrial processes such as electroplating, mining extraction, nuclear power, textile industries, pulp and paper processing, battery manufacturing, and pesticides result in the accumulation of heavy metals into wastewater streams (Akpor et al., 2014; Hubicki & Kołodyńska, 2012). There are many physical and chemical methods available for heavy metal removal in wastewater, however, there are several limitations (Kurniawan et al., 2006). The use of chemical precipitation and coagulation-flocculation in the removal of heavy metals requires large amounts of chemicals to reduce metal concentrations to an acceptable discharge level (Jüttner et al., 2000; Kurniawan et al., 2006). An additional limitation is the production of excessive sludge which is costly to dispose of and requires further treatment (Ayoub et al., 2001; Bose et al., 2002; Yang et al., 2001). Moreover, the use of membrane filtration creates fouling problems due to small membrane pores (Kurniawan et al., 2006; Potts et al., 1981). Any cations present within the contaminated wastewater promotes possibly irreversible membrane fouling (Kurniawan et al., 2006; Potts et al., 1981). A highly fouled membrane

reduces removal efficiencies and must be replaced, therefore, leading to an increase in operational costs (Kurniawan et al., 2006). Additional drawbacks include high energy consumption along with scaling of carbonate species such as  $\text{CaCO}_3$  and  $\text{CaSO}_4$  (Kurniawan et al., 2006).

Compared with other conventional methods mentioned, ion exchange is one of the most widely used methods in addition to membrane filtration for the removal of heavy metals. The main advantage of ion exchange over other conventional techniques is the high selectivity that resins possess towards heavy metals (Kurniawan et al., 2006; Yu et al., 2009). The properties of ion exchange resins can be modified to selectively remove certain ions in solution as the polymeric matrix of the resin can bear a wide variety of functional groups (Crittenden et al., 2012; Zagorodni, 2007). Additional advantages of ion exchange include the high recovery rate of heavy metals and less sludge volume produced compared to chemical precipitation and coagulation-flocculation, therefore resulting in low operational costs for residual sludge disposal (Abo-Farha et al., 2009; Kurniawan et al., 2006; Yu et al., 2009).

Within literature, various studies have focused on the removal of heavy metals using SAC exchange resins. Abo-Farha et al. 2009 demonstrated the removal of  $\text{Ce}^{4+}$ ,  $\text{Fe}^{3+}$ , and  $\text{Pb}^{2+}$  from an initial metal concentration ranging from 2.65-265 mg/L and a resin dosage of 1.0 g/L. Results showed that the maximum percent removal obtained was 86.42%, 80.38%, and 75.47% for  $\text{Ce}^{4+}$ ,  $\text{Fe}^{3+}$ , and  $\text{Pb}^{2+}$ , respectively (Abo-Farha et al., 2009). Studies suggested that ion exchange is dependant on the charge density and the diameter of the hydrated cations (Abo-Farha et al., 2009). Additional studies focused on the removal of

$\text{Cr}^{3+}$  with an initial metal concentration of 10 mg/L and varying resin dosages of 0.5, 1.0, and 1.5 g/L (Rengaraji et al., 2003). Results found that 100% removal efficiency was achieved (Rengaraji et al., 2003). Similar results for  $\text{Cr}^{3+}$  removal were reported by Rengaraji et al. 2001, however, initial metal concentration was increased to 100 mg/L with a resin dosage of 3.0 g/L. In addition, Sapari et al. 1996 studied the removal of  $\text{Zn}^{2+}$  with an initial metal concentration of 5.43 mg/L and achieved a 100% removal rate. Throughout literature, studies have proven that a high removal efficiency can be achieved with the use of SAC exchange resins. However, shortcomings presented in past studies fail to focus on the removal of many heavy metals from a very low initial metal concentration. Therefore, this study will focus on the removal of heavy metals at a metal concentration of 0.1 mg/L using SAC exchange resins.

#### **1.4. Literature Review: ion exchange column**

In ion exchange, there are many techniques used in the removal of contaminants from water and wastewater. These techniques include batch, continuous moving bed, continuous fixed-bed, continuous fluidized bed, and pulsed bed (Patel, 2018; Taty-Costodes et al., 2005). In water and wastewater treatment, a fixed bed column is the most preferable and industrially feasible for the removal of contaminants (Patel, 2018). The performance of a fixed-bed column is described by breakthrough curves (Taty-Costodes et al., 2005). The relation between the nature of breakthrough curves and fixed-bed adsorption is expressed using the mass transfer zone, MTZ (Patel, 2018; Taty-Costodes et al., 2005). In column operation, contaminated feed water flows through the inlet of the column. The

feed water is rapidly adsorbed by the resin bed during the initial stages of operation (Taty-Costodes et al., 2005). This is due to a large amount of resin and a small level of feedwater (Taty-Costodes et al., 2005). As the volume of the contaminated feed water into the column increases, an MTZ becomes defined (Patel, 2018; Taty-Costodes et al., 2005). In this stage of the column, adsorption is complete and the MTZ moves downwards through the column with time until breakthrough occurs (Patel, 2018; Taty-Costodes et al., 2005; Zagorodni, 2007). When the MTZ reaches the bottom of the bed, the contaminated feed water cannot be adsorbed any longer resulting in 'breakpoint' (Patel, 2018; Taty-Costodes et al., 2005; Zagorodni, 2007). The 'breakpoint' is often taken when the effluent concentration becomes 10% of the influent (Taty-Costodes et al., 2005). Once this point has been reached, the bed is completely saturated and the concentration in the column will rapidly increase until saturation point where the effluent concentration is that of the influent concentration (Chartrand, 2018; Wachinski, 2006).

The use of ion exchange columns is used in a wide range of industrial applications. One area of use that will be the focus of this study is in the pretreatment of inorganic cations found within water and wastewater. Membrane processes in water and wastewater treatment face a common problem of mineralization of inorganic solids on the surface of the membrane, known as membrane scaling (Brewster et al., 2017). Scaling occurs when the concentration of low solubility salts exceeds its solubility limit and precipitates on the surface or within membrane structures (Mikhaylin & Bazinet, 2016). In electrodialysis, scaling mostly occurs on the concentrate side of the cation exchange membrane as ion concentrations are the highest due to concentration polarization (Brewster et al., 2017).

Scaling reduction is important to predict and manage as it prevents the migration of ions through the membrane, which significantly increases the membrane stack resistance, therefore, reducing the efficiency of electro dialysis (Brewster et al., 2017). The main ions contributing to scaling in wastewater systems include  $Mg^{2+}$ ,  $Ca^{2+}$ ,  $PO_4^{3-}$ ,  $HCO_3^+$ , and  $CaCO_3$  (Brewster et al., 2017; Mondor et al., 2009). To address the problem of membrane scaling, various techniques have been used such as feed pretreatment using filtration, coagulation-flocculation or acid addition (use of anti-scalant chemicals and/or chemical cleanings) (Brewster et al., 2017; Mondor et al., 2009). Each of these operations requires adding cost and operational downtime in the case of membrane cleaning (Brewster et al., 2017; Greenlee et al., 2009). Due to the limitations of such techniques, the focus will be on developing a one-dimensional ion exchange column model for the pretreatment of inorganic cations to reduce membrane scaling.

## **2. Methodology**

### **2.1. Experimental**

#### **2.1.1. Cation exchange resins**

The resins used throughout the experiments consisted of three various types of SAC exchange resins. The selected resins are used in a wide variety of industrial water and wastewater applications such as water softening, demineralization, and water purification. The physical and chemical properties of the three resins are shown in Table 2.1.

Table 2.1. Strong cation exchange resin properties.

Properties	Resin A <sup>a</sup>	Resin B <sup>a</sup>	Resin C <sup>a</sup>
Polymer Structure <sup>b</sup>	PS/G	PS/G	PS/G
Functional Group	Sulfonate (SO <sub>3</sub> <sup>-</sup> )	Sulfonate (SO <sub>3</sub> <sup>-</sup> )	Sulfonate (SO <sub>3</sub> <sup>-</sup> )
Ionic Form Shipped	Na <sup>+</sup>	Na <sup>+</sup>	H <sup>+</sup>
Crosslinking	8%	8%	16%
Ion Exchange Capacity	≥ 2.0 eq/L	3.8 eq/kg	2.1 eq/L
Moisture Retention	45-50%	36-46%	27-37%
Density	820 g/L	775-825 g/L	865 g/L
Particle Size Range	600-800 μm	300-1200 μm	400-600 μm

<sup>a</sup> Information obtained from manufacturer product data

<sup>b</sup> PS = polystyrene with divinylbenzene, G = gel

Before their use, resins were pretreated using two different solutions: NaCl (1M) or NH<sub>4</sub>Cl (1M). Virgin resins were washed with deionized water (DI) to remove possible organic and inorganic impurities adhered to the surface. Resins were then converted into the Na<sup>+</sup> or NH<sub>4</sub><sup>+</sup> form through 3 batch loading cycles. The pretreatment process was as follows: 20 g of resin was added to 200 mL of NaCl (1M) or NH<sub>4</sub>Cl (1M) and allowed to mix in an Erlenmeyer flask for 1 hour each. For resins shipped in the H<sup>+</sup> form, pH was monitored to ensure the release of H<sup>+</sup> ions from the resin. Once pH became stable, the resin was no longer releasing H<sup>+</sup> ions, therefore, was assumed to be saturated by either Na<sup>+</sup> or NH<sub>4</sub><sup>+</sup>. Following batch cycles, resins were decanted and rinsed with DI water in a sieve. Excess water droplets were removed between resin beads allowing for the resin to be in a ‘wet’ state. This refers to the resin containing enough water inside the bead to be in the fully hydrated state without having excess water between beads (DuPont, 2019). Resins were then stored in an airtight container at room temperature to ensure that resins did not dry and shrink.

### 2.1.2. Equilibrium experiments

Experiments were conducted to study the equilibrium concentrations of various ions within three binary systems: Ca-NH<sub>4</sub>; Ca-Na; and Na-NH<sub>4</sub>. Initial synthetic solutions were prepared with respect to dewatering centrate obtained from Woodward Wastewater Treatment Plant, Hamilton, Ontario. Initial concentrations of solution were chosen to ensure that the equilibrium concentrations of the experiments were comparable to concentrations found in dewatering centrate. The wastewater characteristics of dewatering centrate are shown below in Table 2.2. Synthetic solutions were prepared by dissolving different amounts of CaCl<sub>2</sub> · 2H<sub>2</sub>O, NaCl, NH<sub>4</sub>Cl, and heavy metal plasma standard solution containing Ag<sup>+</sup>, As<sup>3</sup>, Ba<sup>2+</sup>, Cd<sup>2+</sup>, Cr<sup>3+</sup>, Hg<sup>2+</sup>, Pb<sup>2+</sup>, and Se<sup>2-</sup> in DI water. The initial experimental conditions of binary systems studied are summarized in Table 2.3.

Table 2.2: Average wastewater characteristics of Woodward dewatering centrate. (n=3)

Cations	Concentration (mg/L)	Concentration (mM)
NH <sub>4</sub> <sup>+</sup>	1024.2 ± 9.24 (as N)	56.7 ± 0.51(as N)
Na <sup>+</sup>	137.2 ± 10.31	5.97 ± 0.45
Ca <sup>2+</sup>	88.6 ± 8.29	2.21 ± 0.21

Table 2.3: Experimental conditions used for different binary systems studied

Binary Systems	Ionic Form of Resins	Initial Experimental Conditions
Ca-NH <sub>4</sub>	NH <sub>4</sub> <sup>+</sup>	[Ca <sup>2+</sup> ] = 2-24 mM, [NH <sub>4</sub> <sup>+</sup> ] = 40 mM, [H.M] = 0.1 mg/L
Ca-Na	Na <sup>+</sup>	[Ca <sup>2+</sup> ] = 2.5-8 mM, [Na <sup>+</sup> ] = 2-7 mM, [H.M] = 0.1 mg/L
Na-NH <sub>4</sub>	NH <sub>4</sub> <sup>+</sup>	[Na <sup>+</sup> ] = 1.5-25 mM, [NH <sub>4</sub> <sup>+</sup> ] = 40 mM, [H.M] = 0.1 mg/L

The general method used to obtain ion exchange equilibrium data was carried out as follows: 1.0 g of resin and 100 mL of synthetic solution was added to a 250 mL



Erlenmeyer flask. The flasks were sealed and agitated on a flat bed shaker at a speed of 200 rpm for 4 hours to reach equilibrium at constant room temperature ( $22.2 \pm 0.2^\circ\text{C}$ ). The initial pH of the sample solutions ranged from  $5.0 \pm 0.3$  and was adjusted to a neutral pH of  $7.0 \pm 0.2$  using NaOH (1M). Various experimental parameters such as experimental length and resin dosage were determined based on preliminary experiments. At equilibrium, the resins were separated by filtration and regenerated using 100 mL of HCl (1M) solution. The filtrate was subsampled and analyzed. Regeneration was achieved by 4 batch loading cycles in which resins were mixed in an Erlenmeyer flask for 4 hours each. Following the regeneration process, resins were separated by filtration and the filtrate was analyzed. All experiments were performed in duplicates and the results were the averaged value. The concentration of ions in the resin phase at equilibrium was determined from the initial and equilibrium concentrations in the aqueous phase and the known volume and resin mass as shown by Equation (2.1).

$$q_e = \frac{(c_0 - c_e) \cdot v}{m} \quad (2.1)$$

where  $q_e$  (mmol/g) is the resin phase equilibrium concentration,  $c_0$  and  $c_e$  (mM) are the initial and equilibrium aqueous phase ion concentrations and  $v$  (100 mL) and  $m$  (1.0 g) are volume and the resin mass, respectively.

To determine the resin phase concentration of an ion ( $\text{Na}^+$ ,  $\text{NH}_4^+$ ) at equilibrium for a resin saturated by ( $\text{Na}^+$ ,  $\text{NH}_4^+$ ), a mass balance equation can be written as follows:

$$q_e = c_0 \cdot v + q_0 \cdot m - c_e \cdot v \quad (2.2)$$

where  $q_0$  (mmol/g) indicates the initial resin phase concentration and is equivalent to IEC.

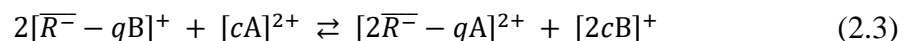
### 2.1.3. Analytical methods

Calcium, sodium, and heavy metal concentrations were measured using ICP-OES (inductively coupled plasma-optical emission spectrometry, Varian Vista Pro). In addition, ammonium ions were measured by analyzing the ammonia nitrogen concentration using high range HACH vials (TNTplus 832). Vials were prepared following the salicylate method described by HACH and were analyzed using a spectrophotometer instrument (HACH DR/2800). The pH of the experimental samples was measured using a pH meter (SevenMulti, Mettler-Toledo International Inc., OH)

## 2.2. Determination of ion exchange capacity and selectivity coefficient

The purpose of this section was to develop a linear system for determining ion exchange equilibria parameters through plotting experimental data. A linear least-square fitting was employed to find representative IEC and K values covering various resins and experimental conditions. Within the following subsections, two linear models have been developed to investigate IEC and K values of three binary systems: Ca-NH<sub>4</sub>; Ca-Na; and Na-NH<sub>4</sub>.

The determination of IEC and K parameters was carried out using a binary system in which a divalent ion, A<sup>2+</sup> present in an aqueous solution is exchanged with a monovalent ion, B<sup>+</sup> from the resin. The ion exchange reaction can be represented as:



where  $\overline{R}^-$  is the active site on the resin backbone, A and B are the exchangeable counterions and  $c$  (mM) and  $q$  (mmol/g) are aqueous and resin phase concentrations. Reaction (2.3) yields the selectivity coefficient expression:

$$K_{A/B} = \frac{(q_A) \cdot (c_B)^2}{(c_A) \cdot (q_B)^2} \quad (2.4)$$

where  $K_{A/B}$  is the selectivity coefficient for the preference of species A over species B. According to Equation (2.4), the preference for species A over species B leads to the numerical value of  $K_{A/B} > 1$ . If species B is more preferred by the resin, the value will be  $< 1$ . The sites within the resin are assumed to always be fully occupied with either species A or B, therefore, the following equation can be written:

$$IEC = 2q_A + q_B \quad (2.5)$$

### 2.2.1. Linearization Method #1

The determination of IEC and  $K_{A/B}$  are carried out by combining the governing equations of ion exchange defined in Equations (2.4) and (2.5) as developed in Section 2.2, therefore, obtaining Equation (2.6).

$$K_{A/B} = \frac{(q_A) \cdot (c_B)^2}{(c_A) \cdot (IEC - 2q_A)^2} \quad (2.6)$$

IEC and  $K_{A/B}$  are unknown parameters in the linear system and  $c_A$ ,  $q_A$ , and  $(c_B)^2$  are constants. To solve for IEC and  $K_{A/B}$ , Equation (2.6) can be rearranged to give the following equation:

$$\frac{1}{(K_{A/B})^{1/2}} = \frac{(c_A)^{1/2}}{(q_A)^{1/2} \cdot (c_B)} \cdot (IEC - 2q_A) \quad (2.7)$$

Equation (2.7) can be converted into Equation (2.8) by expanding the two expressions on the right-hand side of the equation and simplifying it. The constant variables within the model;  $c_A$ ,  $q_A$ , and  $(c_B)^2$  are to be treated as one entity when expanding.

$$2q_A \cdot \frac{(c_A)^{1/2}}{(q_A)^{1/2} \cdot (c_B)} = IEC \cdot \frac{(c_A)^{1/2}}{(q_A)^{1/2} \cdot (c_B)} - \frac{1}{(K_{A/B})^{1/2}} \quad (2.8)$$

IEC and  $K_{A/B}$  can be determined through linear least-square fitting by plotting  $\frac{(c_A)^{1/2}}{(q_A)^{1/2} \cdot (c_B)}$  versus  $\frac{(2q_A)(c_A)^{1/2}}{(q_A)^{1/2} \cdot (c_B)}$ , which is linearly correlated with a unit slope and y-intercept of IEC (eq/L) and  $-\frac{1}{(K_{A/B})^{1/2}}$  (g/L), respectively as written in Equation (2.8).

### 2.2.2. Linearization Method #2

The determination of IEC and  $K_{A/B}$  are carried out by combining the governing equations of ion exchange defined in Equations (2.4) and (2.5) developed in Section 2.2, therefore, obtaining Equation (2.6) in Section 2.2.1. To solve for IEC and  $K_{A/B}$ , Equation (2.6) can be rearranged to yield the following equation:

$$\frac{(q_A)^{1/2} \cdot (c_B)}{(c_A)^{1/2}} = (K_{A/B})^{1/2} (IEC - 2q_A) \quad (2.9)$$

Equation (2.9) can be rearranged to give the following equation:

$$\frac{(q_A)^{1/2} \cdot (c_B)}{(c_A)^{1/2}} = -2q_A(K_{A/B})^{1/2} + \text{IEC}(K_{A/B})^{1/2} \quad (2.10)$$

IEC and  $K_{A/B}$  can be determined through linear least-square fitting by plotting  $2q_A$  versus  $\frac{(q_A)^{1/2} \cdot (c_B)}{(c_A)^{1/2}}$ , which is linearly correlated with a unit slope and y-intercept of  $(K_{A/B})^2$  (eq/L),  $\frac{\text{IEC}}{(K_{A/B})^{1/2}}$  (g/L), respectively as written in Equation (2.10).

### 2.3. Ion exchange column model development

The one-dimensional equilibrium model developed in this section simulates the non-steady ionic exchange in a column reactor. The objective of the model is to develop a pretreatment method reducing membrane scaling. An assumption of this model is instantaneous equilibrium between both the aqueous and resin phases. The column can be modelled by the differential mass balance of solute transport in a segment of the column, illustrated in Figure 2.1. The governing equation that includes the rate of ion exchange within a single resin particle is represented by the following one-dimensional equation:

$$V(c_{\text{in}}^{n-1} - c_{\text{out}}^n) = (\Delta Z)(\varepsilon) \left( \frac{dc}{dt} \right) + (\Delta Z)(1 - \varepsilon)(\rho) \left( \frac{dq}{dt} \right) \quad (2.11)$$

where  $V$ ,  $\Delta Z$ ,  $\varepsilon$  and  $\rho$  represent flow velocity (cm/min), grid thickness (cm), porosity, and resin density (g/L), respectively.  $c_{\text{in}}$  and  $c_{\text{out}}$  represent concentration entering and exiting a specific grid within the column. The superscripts  $n$  and  $n-1$  denote the column grid number and  $\frac{dc}{dt}$  (mM) and  $\frac{dq}{dt}$  (mmol/g) represent the rate of ion exchange in the aqueous

and resin phases, respectively. Equation (2.11) can be written for both  $\text{Ca}^{2+}$  and  $\text{NH}_4^+$  in the aqueous and resin phases.

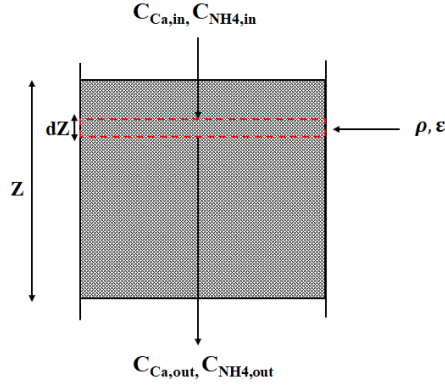


Figure 2.1: Schematic diagram for the mass balance of a solute in a segment of a column.

The backwards difference method in  $Z$ , was used to convert the differential equation defined in Equation (2.11) into the algebraic mass balance difference equation as follows:

$$V(c_{in}^{n-1} - c_{out}^n) = (dZ)(\varepsilon) \left( \frac{c^{t+1} - c^t}{\Delta t} \right) + (dZ)(1 - \varepsilon)(\rho) \left( \frac{q^{t+1} - q^t}{\Delta t} \right) \quad (2.12)$$

where superscript  $t$  and  $t+1$  denote the time steps within the column

To solve the mass balance defined in Equation (2.12), the equations for  $K_{A/B}$  and IEC defined in Section 2.2 can be rearranged as follows:

$$q_{Ca}^{t+1} = \frac{(K_{Ca/NH_4}) \cdot (c_{NH_4}^{t+1})^2 \cdot (c_{Ca}^{t+1})}{(q_{NH_4}^{t+1})^2} \quad (2.13)$$

$$q_{NH_4}^{t+1} = IEC - 2q_{Ca}^{t+1} \quad (2.14)$$

The mass balance represented in Equation (2.12) can be rearranged for  $\text{Ca}^{2+}$  and  $\text{NH}_4^+$  in the aqueous phase as follows:

$$c_{\text{out,Ca}} = \frac{(V)(\Delta t)(c_{\text{in,Ca}}) + (\Delta Z)(\varepsilon)(c_{\text{Ca}}^t) - (\rho)(\Delta Z)(1 - \varepsilon)(q_{\text{Ca}}^{t+1} - q_{\text{Ca}}^t)}{(\Delta Z)(\varepsilon) + (V)(\Delta t)} \quad (2.15)$$

$$c_{\text{out,NH}_4} = \frac{(V)(\Delta t)(c_{\text{in,NH}_4}) + (\Delta Z)(\varepsilon)(c_{\text{NH}_4}^t) - (\rho)(\Delta Z)(1 - \varepsilon)(q_{\text{NH}_4}^{t+1} - q_{\text{NH}_4}^t)}{(\Delta Z)(\varepsilon) + (V)(\Delta t)} \quad (2.16)$$

Equations (2.13) and (2.14) can be combined with Equations (2.15) and (2.16) and solved using fixed-point iteration numerical method. A convergence criterion with an absolute error of  $10^{-4}$  was used to solve the system of nonlinear equations. The non-steady state model was implemented using operational parameters in Table 2.4 and coded using visual basic application (VBA).

Table 2.4: Initial model parameters for a one-dimensional ion exchange column.

Model Parameters			
$c_{\text{Ca,in}}$	3 mM	$\Delta Z$	40 grids- 2 cm/grid
$c_{\text{NH}_4,\text{in}}$	40 mM	$\rho$	1270 g/L
$q_{\text{Ca}}$	0 mmol/g	$V$	20 cm/min
$q_{\text{NH}_4}$	2 mmol/g	$Z$	80 cm
$\Delta t$	0.50 min	$\varepsilon$	0.4

### 3. Results and Discussion

#### 3.1. Determination of IEC and $K_{\text{Ca}/\text{NH}_4}$ by linearization Method #1

The IEC values determined from the slope of the linear equation using Method 1, Equation (2.8) are 2.29 (Resin A), 1.96 (Resin B), and 2.05 eq/L (Resin C). The IEC values obtained from Figure 3.1 (A) and (C) are in agreement with the IEC values stated by the

manufacturer in Section 2.1.1. In Figure 3.1 (B), the IEC value is not comparable with the manufacturer value of 3.04 eq/L. The  $K_{Ca/NH_4}$  values obtained from the y-intercept of the linear equation using Method 1, Equation (2.8) are 2.45 (Resin A), 2.42 (Resin B), and 3.23 kg-resin/L-solution (Resin C).

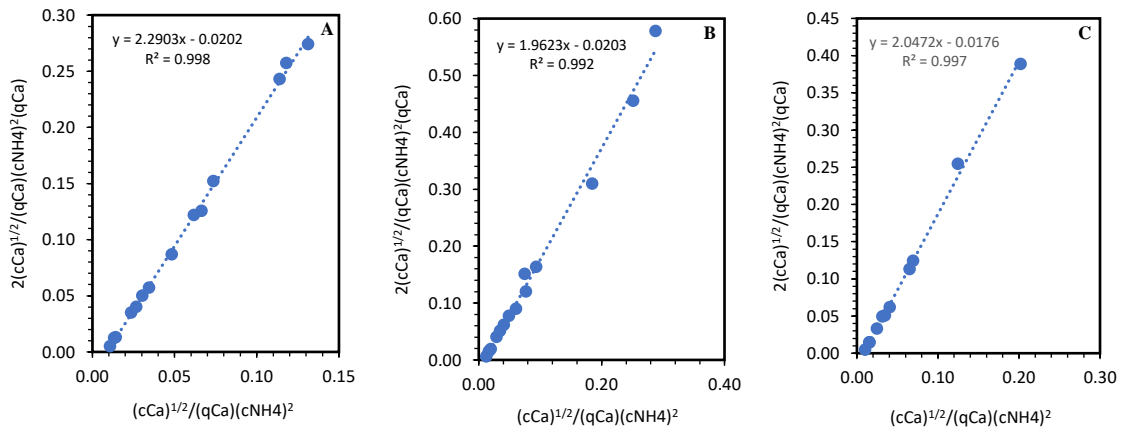


Figure 3.1: Determination of IEC and K for Ca-NH<sub>4</sub> system: (A) Resin A; (B) Resin B; (C) Resin C.

### 3.2. Determination of IEC and $K_{Ca/NH_4}$ by linearization Method #2

The IEC values determined from the y-intercept of the linear equation using Method 2, Equation (2.10) are 2.26 (Resin A), 1.92 (Resin B), and 2.01 eq/L (Resin C). The values are consistent with reported IEC values in Section 3.1. The obtained IEC values from Figure 3.2 (A) and (C) are in agreement with the IEC values stated by the manufacturer in Section 2.1.1. The IEC values according to the manufacturer are  $\geq 2$  eq/L for Resin A and 2.1 eq/L for Resin C. In Figure 3.2 (B), to compare the determined IEC value of 1.96 eq/L with the manufacturer value, units need to be converted by multiplying the IEC value of 3.8 eq/kg by the average density reported by the manufacturer of 0.8 kg/L. Therefore, resulting in an



IEC value of 3.04 eq/L. This value is not consistent with the obtained IEC values using Methods 1 and 2. A possible reason for an apparent decrease in IEC may be due to the inaccuracy of characterization tests performed by the manufacturer. This can be assumed as typical reported IEC values for SAC exchange resins range from 1.7-2.1 eq/L (Crittenden et al., 2012). The  $K_{Ca/NH_4}$  values determined from the slope of the linear equation using Method 2, Equation (2.10) are 2.82 (Resin A), 2.87 (Resin B), and 3.54 kg-resin/L-solution (Resin C).

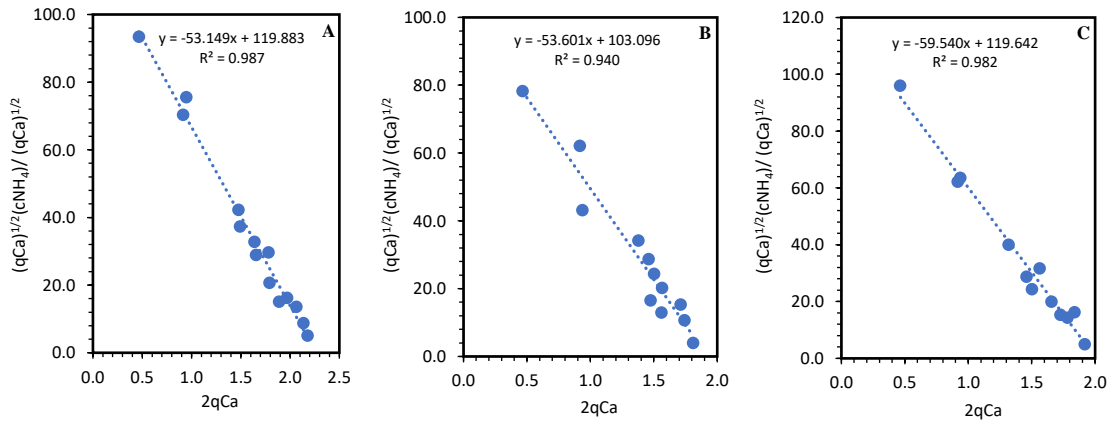


Figure 3.2: Determination of IEC and K for Ca-NH<sub>4</sub> system: (A) Resin A; (B) Resin B; (C) Resin C.

### 3.3. Propagation of small analytical errors in the two linearization methods

The developed linearization methods in Sections 2.2.1 and 2.2.2 were analyzed for stability. A summary of IEC and  $K_{Ca/NH_4}$  values for all three resin types studied are outlined in Table 3.1. Using Methods 1 and 2,  $Ca_0$  concentration data points were omitted from highest to lowest ranging from 24 mM to 2.5 mM. IEC and  $K_{Ca/NH_4}$  were determined each

time a data point was omitted, resulting in 10 new IEC and  $K_{Ca/NH_4}$  values. The average ( $\bar{X}$ ) and standard deviation ( $\sigma$ ) of the calculated IEC and  $K_{Ca/NH_4}$  are reported in Table 3.1.

Table 3.1: Effect of variation in Methods 1 and 2 on (A) IEC (eq/L); (B)  $K_{Ca/NH_4}$  (kg/L) for Resins A, B, C.

(A)

Resin A		Resin B		Resin C	
M1	M2	M1	M2	M1	M2
2.294	2.277	1.955	1.901	2.160	2.006
2.268	2.277	1.995	1.918	2.171	2.007
2.245	2.269	1.992	1.960	1.969	1.967
2.247	2.288	1.762	1.992	1.953	1.985
2.231	2.271	2.069	2.008	1.986	2.000
2.266	2.306	1.938	2.014	2.004	2.013
2.266	2.310	1.938	2.005	2.103	2.037
2.276	2.314	1.939	1.990	2.139	2.071
2.276	2.287	1.950	2.017	1.799	2.086
2.248	2.301	1.941	1.954	1.864	2.105
$\bar{X}=2.261$	$\bar{X}=2.290$	$\bar{X}=1.948$	$\bar{X}=1.976$	$\bar{X}=2.015$	$\bar{X}=2.028$
$\sigma=0.019$	$\sigma=0.017$	$\sigma=0.077$	$\sigma=0.041$	$\sigma=0.127$	$\sigma=0.046$

(B)

Resin A		Resin B		Resin C	
M1	M2	M1	M2	M1	M2
2.525	2.739	2.657	2.990	2.066	3.566
2.713	2.738	2.268	2.909	2.047	3.560
2.891	2.777	2.525	2.694	3.810	3.861
2.986	2.706	0.113	2.588	4.006	3.764
2.986	2.784	2.334	2.510	3.764	3.692
2.713	2.706	3.121	2.489	3.718	3.613
2.799	2.677	3.121	2.520	3.019	3.471
2.799	2.659	3.019	2.587	2.922	3.320
2.829	2.758	2.954	2.390	5.176	3.379
2.954	2.709	2.891	2.648	4.691	3.426
$\bar{X}=2.820$	$\bar{X}=2.725$	$\bar{X}=2.500$	$\bar{X}=2.632$	$\bar{X}=3.522$	$\bar{X}=3.565$
$\sigma=0.145$	$\sigma=0.041$	$\sigma=0.895$	$\sigma=0.188$	$\sigma=1.023$	$\sigma=0.173$

For Method 1, IEC values for Resins A-C deviated 0.019, 0.077, and 0.127 when omitting data points from highest to lowest  $Ca_0$  concentrations. For Method 2, IEC values deviated 0.017, 0.041 and 0.046 for Resins A-C, respectively when omitting data points from highest to lowest  $Ca_0$  concentrations. The trends show that both methods used to calculate IEC are stable, as slight deviations ( $< 0.13$ ) were observed amongst both methods, therefore, resulting in a minimal fluctuation of IEC values when data points were omitted.

In addition,  $K_{Ca/NH_4}$  values were compared amongst Methods 1 and 2. For Method 1,  $K_{Ca/NH_4}$  values for Resins A-C deviated 0.145, 0.895, and 1.023 when omitting data points from highest to lowest  $Ca_0$  concentrations. The calculated standard deviations show that  $K_{Ca/NH_4}$  is an unstable parameter as fluctuations in  $K_{Ca/NH_4}$  were observed when data points were omitted. This shows that the determination of  $K_{Ca/NH_4}$  using Method 1 is dependant on the calculation method chosen (slope or y-intercept). In Method 2,  $K_{Ca/NH_4}$  values deviated 0.041, 0.188, and 0.173 for Resins A-C, respectively. This trend shows that  $K_{Ca/NH_4}$  is a stable parameter as minimal fluctuations in  $K_{Ca/NH_4}$  were observed when data points were omitted. Due to the stable nature of Method 2, the determination of IEC and K for additional binary systems will be calculated using this method.

### **3.4. Determination of IEC and $K_{Ca/Na}$ by linearization Method #2**

The IEC values determined from the y-intercept of the linear equation using Method 2, Equation (2.10) are 2.06 (Resin A), 2.08 (Resin B), and 2.03 eq/L (Resin C). The obtained IEC values from Figure 3.3 (A) and (C) are in agreement with the IEC values

stated by the manufacturer in Section 2.1.1. In Figure 3.4 (B), the determined IEC value of 2.08 eq/L is not consistent with the reported manufacturer value of 3.04 eq/L. The observed trends are consistent with the IEC values obtained in Section 3.2.

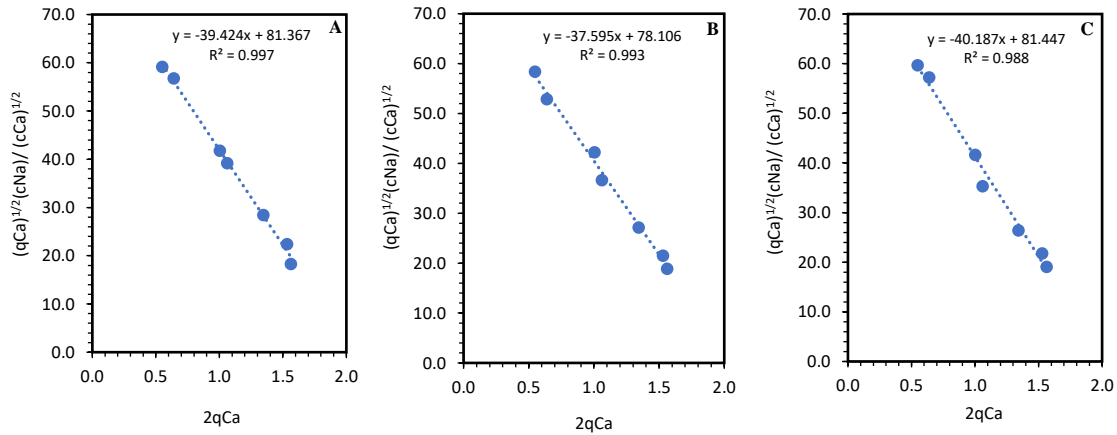


Figure 3.3: Determination of IEC and K for Ca-Na system: (A) Resin A; (B) Resin B; (C) Resin C.

Variations in IEC values of binary systems Ca-NH<sub>4</sub> and Ca-Na are observed in Sections 3.2 and 3.4 using Method 2. An explanation for the observed variation is due to the dependency on which IEC has upon the moisture content of the resin (Crittenden et al., 2012). The moisture content is based on the functional form of the resin, therefore, given two different ion forms of the same resin, IEC will differ due to the differences in water content attributed to resin swelling (Crittenden et al., 2012). Ion exchange depends upon reducing resin swelling, therefore ions containing a smaller hydrated radius are preferred (Crittenden et al., 2012). In this study, resins were saturated into two different ionic forms, NH<sub>4</sub><sup>+</sup> and Na<sup>+</sup>. The hydrated radii of both cations are 3.31 Å and 3.58 Å, respectively. (Nightingale, 1959). According to the definition of IEC defined as the number of functional groups within the ion exchange resin, it is assumed that a resin saturated with NH<sub>4</sub><sup>+</sup> should

result in a greater number of functional groups. This is due to  $\text{NH}_4^+$  having a smaller hydrated radius resulting in a decrease in resin swelling (Crittenden et al., 2012). The  $K_{\text{Ca}/\text{Na}}$  determined from the slope of the linear equation using Method 2, Equation (2.10) are 1.55 (Resin A), 1.41 (Resin B), and 1.61 kg-resin/L-solution (Resin C).

### 3.5. Selectivity of divalent over monovalent cations

Variations observed between  $K_{\text{Ca}/\text{NH}_4}$  values outlined in Section 3.2, are attributed to the increase in crosslinking. Similar trends are observed in  $K_{\text{Ca}/\text{Na}}$  values outlined in Section 3.4; however, a reduced variability is observed in  $K_{\text{Ca}/\text{Na}}$ . Resins A and B both have a nominal percent crosslinking of 8% in comparison to Resin C which has a nominal percent crosslinking of 16%. The degree of crosslinking governs the extent of resin swelling (Crittenden et al., 2012; Harland, 1994; Zagorodni, 2007). Resin crosslinking provides the fundamental chemical bonding between adjacent polymer chains giving the resin its inherent physical strength (Harland, 1994). Therefore, with an increase in crosslinking, percent resin swelling decreases as highly crosslinked resins are more rigid (Crittenden et al., 2012; Harland, 1994; Zagorodni, 2007). The reduction in resin swelling allows for active sites within the resin to be closer together, therefore, allowing the resin to exhibit a higher ionic strength leading to a stronger attraction for the preferred ion (Crittenden et al., 2012; Zagorodni, 2007). The results from the obtained  $K_{\text{Ca}/\text{NH}_4}$  and  $K_{\text{Ca}/\text{Na}}$  values are consistent with previous selectivity coefficient studies, as literature has reported that crosslinking is directly linked to the selectivity of an ion (Jackson & Bolto, 1990).

From the obtained  $K_{Ca/NH_4}$  and  $K_{Ca/Na}$  using Method 2, it is apparent that  $Ca^{2+}$  is preferred by the resin over  $NH_4^+$  and  $Na^+$ . In ion exchange, resin selectivity is influenced by the degree of swelling or pressure within the resin bead (Crittenden et al., 2012). The preference of one ionic species over another is attributed to the electrostatic interaction between the charged framework and the counterion. Therefore, the preference of one counterion over another is governed by the valence and the hydrated radius (Crittenden et al., 2012; Zagorodni, 2007). Ion exchange resins prefer counterions with a higher ionic charge as it results in reduced resin swelling (Abo-Fartha et al., 2009; Crittenden et al., 2012; Rengaraji et al., 2003). In addition, counterions with a smaller hydrated radius result in a higher affinity by the resin (Crittenden et al., 2012). This trend is directly correlated to resin swelling as ions with a smaller hydrated radius are more easily accommodated into the resin pores (Crittenden et al., 2012; Zagorodni, 2007).

### **3.6. Competition between $Na^+$ and $NH_4^+$**

The determination of  $K_{Na/NH_4}$  was accomplished from the slope of the linear equation by plotting  $q_{NH_4}/c_{NH_4}$  versus  $q_{Na}/c_{Na}$  and setting the y-intercept equal to zero. The experimentally obtained  $K_{Na/NH_4}$  values in Figure 3.4 are 1.09 (Resin A), 1.08 (Resin B), and 1.10 (Resin C). The calculated  $K_{Na/NH_4}$  values determined by dividing  $K_{Ca/NH_4}$  by  $K_{Ca/Na}$  are 1.83 (Resin A), 2.04 (Resin B), and 2.20 (Resin C). Both  $K_{Na/NH_4}$  values determined through experiments and calculations are comparable with  $K_{Na/NH_4}$  values observed in literature (Marinsky, 1966).

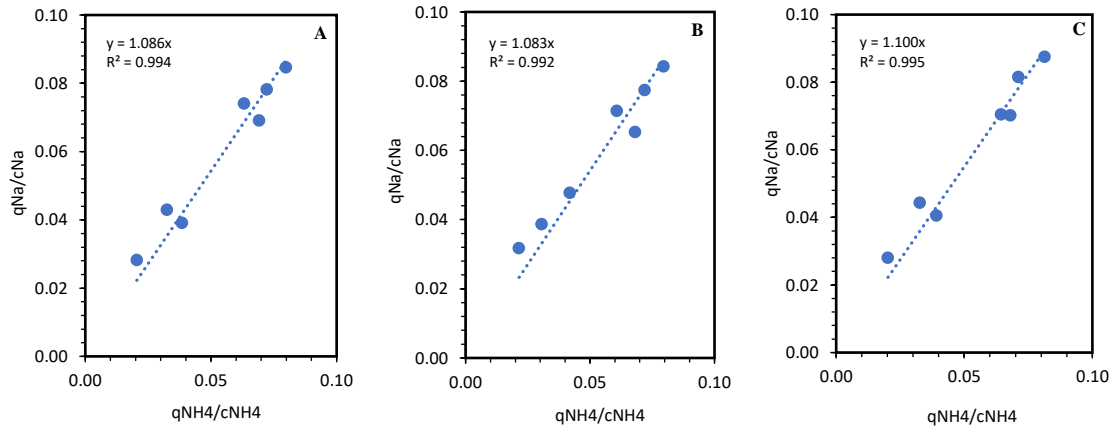


Figure 3.4: Determination of K for Na-NH<sub>4</sub> system: (A) Resin A; (B) Resin B; (C) Resin C.

The competition between Na<sup>+</sup> and NH<sub>4</sub><sup>+</sup> can be compared in the three binary systems studied: Ca-NH<sub>4</sub>; Ca-Na; and Na-NH<sub>4</sub>. As mentioned in Section 3.5, the preference of one ionic species over another is governed by the size of the hydrated radius of the counterion (Crittenden et al., 2012; Zagorodni, 2007). Ion exchange resins prefer counterions with a smaller hydrated radius as they are more easily accommodated into resin pores, therefore, reducing resin swelling (Crittenden et al., 2012; Zagorodni, 2007). In comparing the hydrated radii of Na<sup>+</sup> and NH<sub>4</sub><sup>+</sup> the values are as follows: 3.58 Å and 3.31 Å, respectively (Nightingale, 1959). In the obtained  $K_{Ca/NH_4}$  and  $K_{Ca/Na}$  outlined in Sections 3.2 and 3.4, the system Ca-NH<sub>4</sub> shows greater selectivity towards Ca<sup>2+</sup> compared to the Ca-Na system. Based on the theory of hydrated radii,  $K_{Ca/Na}$  should possess a greater selectivity towards Ca<sup>2+</sup> compared to  $K_{Ca/NH_4}$ . This is due to Na<sup>+</sup> having a greater hydrated radius compared to NH<sub>4</sub><sup>+</sup>, therefore, resulting in Na<sup>+</sup> to not be as easily accommodated into the resin pores as compared to NH<sub>4</sub><sup>+</sup>. In the Na-NH<sub>4</sub> system, experimental and calculated  $K_{Na/NH_4}$  values show that Na<sup>+</sup> is preferred by the resin over

$\text{NH}_4^+$ . Ideally, based on theory,  $\text{NH}_4^+$  should be more preferred by the resin over  $\text{Na}^+$  as the hydrated radius is smaller. These results show that the affinity by the resin for a counterion is not only governed by valency and hydrated radii but also by concentration. In the study between  $\text{Na}^+$  and  $\text{NH}_4^+$ , resins were saturated with  $\text{NH}_4^+$ . As resins encounter high concentrations of  $\text{Na}^+$  in the aqueous phase, a large concentration gradient exists between the aqueous phase and the resin interface. This leads to a significant drive for  $\text{Na}^+$  to diffuse into the resin interface, therefore, showing that counterions of a larger hydrated radius have the ability to be more preferred by the resin at high concentrations. Further studies on the competitive nature between  $\text{Na}^+$  and  $\text{NH}_4^+$  are required for a clear understanding of the ion exchange reactions.

In monovalent systems, the degree of crosslinking plays a limited role in the variation of selectivity compared to divalent systems observed in Sections 3.2 and 3.4. Marinsky (1966) and Phipps and Hume (1967) observed similar trends in evaluating the effect of percent crosslinking on selectivity coefficients of monovalent systems. Both studies observed minimal selectivity variation with an increase in nominal percent crosslinking (Marinsky, 1966; Phipps & Hume, 1967).

### **3.7. Heavy metal removal**

Heavy metal removal using SAC exchange resins was investigated on various binary systems: Na- $\text{NH}_4$ ; Ca- $\text{NH}_4$ ; and Ca-Na. Three resin types were studied, and results were averaged representing percent removal of heavy metals outlined in Figure 3.5. The results show that SAC exchange resins effectively removed  $\text{Cr}^{3+}$ ,  $\text{Pb}^{2+}$ ,  $\text{Ba}^{2+}$ , and  $\text{Cd}^{2+}$  from



an initial heavy metal concentration of 0.1 mg/L. The maximum percent removal in all three binary systems studied ranged from ~ 97-99% for  $\text{Cr}^{3+}$ ,  $\text{Pb}^{2+}$ ,  $\text{Ba}^{2+}$ , and ~ 95% for  $\text{Cd}^{2+}$ . A low percent removal was observed for both  $\text{Hg}^{2+}$  and  $\text{Ag}^+$  in all three binary systems studied. The maximum percent removal observed for  $\text{Hg}^{2+}$  and  $\text{Ag}^+$  was ~ 7% and ~ 17%, respectively. The low percent removal is attributed to the presence of  $\text{Cl}^-$  in solution as both metal cations form insoluble precipitates with  $\text{Cl}^-$ . Moreover, anionic heavy metals,  $\text{As}^{3-}$  and  $\text{Se}^{2-}$  were not removed using SAC exchange resins in all three binary systems studied. This trend is due to the matrix of SAC exchange resins in which a negatively charged sulfonate group is permanently fixed to the resin, giving a negatively charged matrix (Crittenden et al., 2012). Associated with these negatively charged groups are mobile counterions which are of opposite charge to the functional groups (Crittenden et al., 2012). In SAC exchange resins, counterions are cations therefore, leading to the minimal percent removal of anions observed in solution. Heavy metal concentration limits found in municipal wastewater effluent are shown in Table 3.2. This table outlines the benchmark concentration limits established by CCME for municipal wastewater effluent discharged into freshwater environments. The benchmark limits were established for the protection of human water use and ecological health (CCME, 2006). The treated heavy metal effluent outlined in Figure 3.5 satisfies the regulated CCME concentration limits for both  $\text{Cd}^{2+}$  and  $\text{Cr}^{3+}$ . It is to be noted that the values outlined in Table 3.2 vary from the Model Sewer Use Bylaw Limit presented by CCME, 2009, therefore, leading to  $\text{Ag}^+$ ,  $\text{Pb}^{2+}$ ,  $\text{Cd}^{2+}$ , and  $\text{Cr}^{3+}$  satisfying regulated concentrations.

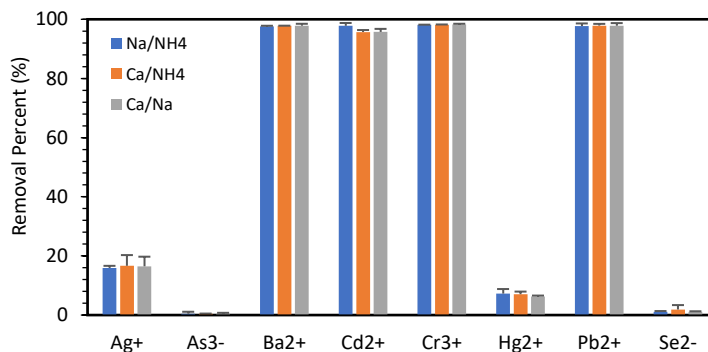


Figure 3.5: Percent removal of heavy metals from various binary systems. (results based on the average and standard deviation)

Table 3.2: Heavy metal concentration limits found in municipal wastewater effluent.

Heavy Metal Ions	CCME Concentration Limit ( $\mu\text{g/L}$ ) <sup>a</sup>
Ag <sup>+</sup>	5
As <sup>3-</sup>	1000
Ba <sup>2+</sup>	0.97
Cd <sup>2+</sup>	8.9
Cr <sup>3+</sup>	7
Hg <sup>2+</sup>	0.16
Pb <sup>2+</sup>	0.1
Se <sup>2-</sup>	1

<sup>a</sup> Canadian Council of Ministers of the Environment (CCME), 2006

An important aspect of this study is the high percent removal of toxic heavy metals, Cr<sup>3+</sup>, Pb<sup>2+</sup>, Ba<sup>2+</sup>, and Cd<sup>2+</sup> from a solution containing a low molar concentration of heavy metals and a high molar concentration of Ca<sup>2+</sup>, Na<sup>+</sup>, and NH<sub>4</sub><sup>+</sup>. In the three binary systems studied, the molar concentrations in solution included Cr<sup>3+</sup> (0.00192 mM), Pb<sup>2+</sup> (0.00048 mM), Ba<sup>2+</sup> (0.00073 mM), Cd<sup>2+</sup> (0.00089 mM), Ca<sup>2+</sup> (1.5-25 mM), Na<sup>+</sup> (2-7 mM), and NH<sub>4</sub><sup>+</sup> (40 mM). SAC exchange resins were responsible for ~ 95-99% removal of the toxic heavy metal ions. The results show the ability of SAC exchange resins to effectively remove toxic heavy metals at very low molar concentrations. The high selectivity that SAC

exchange resins possess towards heavy metals proves that they can be used as a pretreatment method for the removal of toxic heavy metals from municipal and industrial wastewaters. In addition to pretreatment, ion exchange resins have high metal recovery value due to the ability of ion exchange resins to be regenerated once equilibrium has been achieved (Abo-Farha et al., 2009; Kurniawan et al., 2006). This allows ion exchange to be very advantageous in heavy metal removal over other common methods.

### **3.8. One-dimensional column model**

#### **3.8.1. Concentration time profile of $\text{Ca}^{2+}$ and $\text{NH}_4^+$**

In the one-dimensional ion exchange column, a model was created to simulate the removal of  $\text{Ca}^{2+}$  from a feed solution containing 3 mM of  $\text{Ca}^{2+}$  and 40 mM of  $\text{NH}_4^+$ . The resin bed contains SAC exchange resins which are initially saturated with  $\text{NH}_4^+$ . Additional parameters used in the model are represented in Section 2.3, Table 2.4. Figure 3.6 depicts the concentration profiles of  $\text{Ca}^{2+}$  and  $\text{NH}_4^+$  as a function of time. As the initial feed solution is passed through the column,  $\text{Ca}^{2+}$  is most rapidly exchanged by the upper layers of the resin bed during the initial stages. This is due to the higher amounts of resin compared to  $\text{Ca}^{2+}$  concentration. The MTZ is attained near the top of the column. During this stage in the column,  $\text{Ca}^{2+}$  concentration is zero, as the slope of the effluent  $\text{Ca}^{2+}$  is equal to zero. When  $\text{Ca}^{2+}$  concentration is zero,  $\text{NH}_4^+$  concentration increases until reaching its highest point at 4.5 minutes. This is due to the resin being initially saturated with  $\text{NH}_4^+$ , therefore, with an increase in  $\text{Ca}^{2+}$  into the resin, an increase of  $\text{NH}_4^+$  into feed solution is observed. When the MTZ reaches the bottom of the column,  $\text{Ca}^{2+}$  can no longer be exchanged

resulting in the column reaching its breakpoint. The breakpoint is observed at 7.5 minutes and is represented at the point where the effluent  $\text{Ca}^{2+}$  concentration becomes 10% of the influent (Taty-Costodes et al., 2005). Once the breakpoint has been reached, the column is completely saturated (Patel, 2019; Taty-Costodes et al., 2005). This is attributed to the concentration of  $\text{Ca}^{2+}$  increasing rapidly until the effluent concentration is equal to the influent concentration. The saturation point occurs at 31.5 minutes when the slope of  $\text{Ca}^{2+}$  effluent concentration is equal to zero. The results outlined in this section may show the potential overestimation of  $\text{Ca}^{2+}$  uptake by the resin. This is due to the assumption outlined in Section 2.3 in that instantaneous equilibrium occurs between both the aqueous and resin phases within the column.

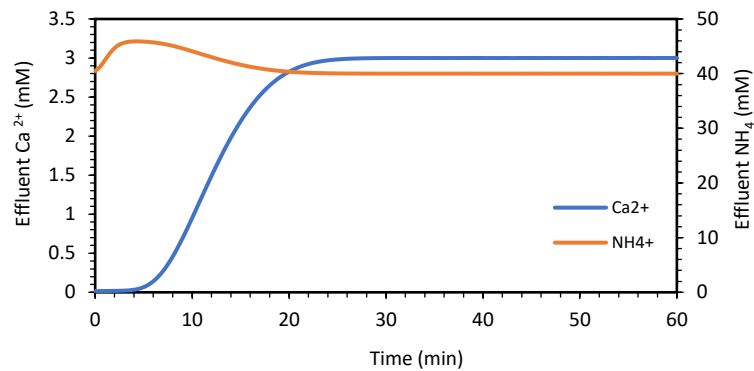


Figure 3.6: Concentration time profile of  $\text{Ca}^{2+}$  and  $\text{NH}_4^+$ .

### 3.8.2. Effect of $K_{Ca/NH_4}$ , IEC, porosity, and velocity on calcium removal

The effect of variation in model parameters,  $K_{Ca/NH_4}$ , IEC, porosity ( $\epsilon$ ), and flow velocity ( $V$ ) on the breakthrough profile of  $Ca^{2+}$  is shown in Figure 3.7 (A-D), respectively. The breakthrough curve of  $Ca^{2+}$  was investigated using various  $K_{Ca/NH_4}$  and IEC values ranging from 0.001-0.01 kg/L and 0.5-2 eq/L, respectively. Additional parameters used in the model are represented in Section 2.3, Table 2.4. The results in Figure 3.7 (A) and (B) indicate that an increase in  $K_{Ca/NH_4}$  and IEC is proportional to an increase in breakthrough time. An increase in both  $K_{Ca/NH_4}$  and IEC has a significant effect on the shape of the breakthrough curve. Any change applied to  $K_{Ca/NH_4}$  and IEC results in a shift in the obtained values for breakthrough time. With an increase in  $K_{Ca/NH_4}$  and IEC within the model, the affinity for  $Ca^{2+}$  by the resin increases. This is evident by the increase in the time needed to achieve breakpoint. An increase in  $K_{Ca/NH_4}$  allows for  $Ca^{2+}$  to occupy more exchange sites compared to  $NH_4^+$  resulting in an increased  $Ca^{2+}$  uptake (Crittenden et al., 2012). Also, an increase in IEC allows for an increase in the number of functional groups available within the resin. This results in the resin bed to not become saturated as rapidly, therefore, leading to an increase in  $Ca^{2+}$  uptake (Crittenden et al., 2012).

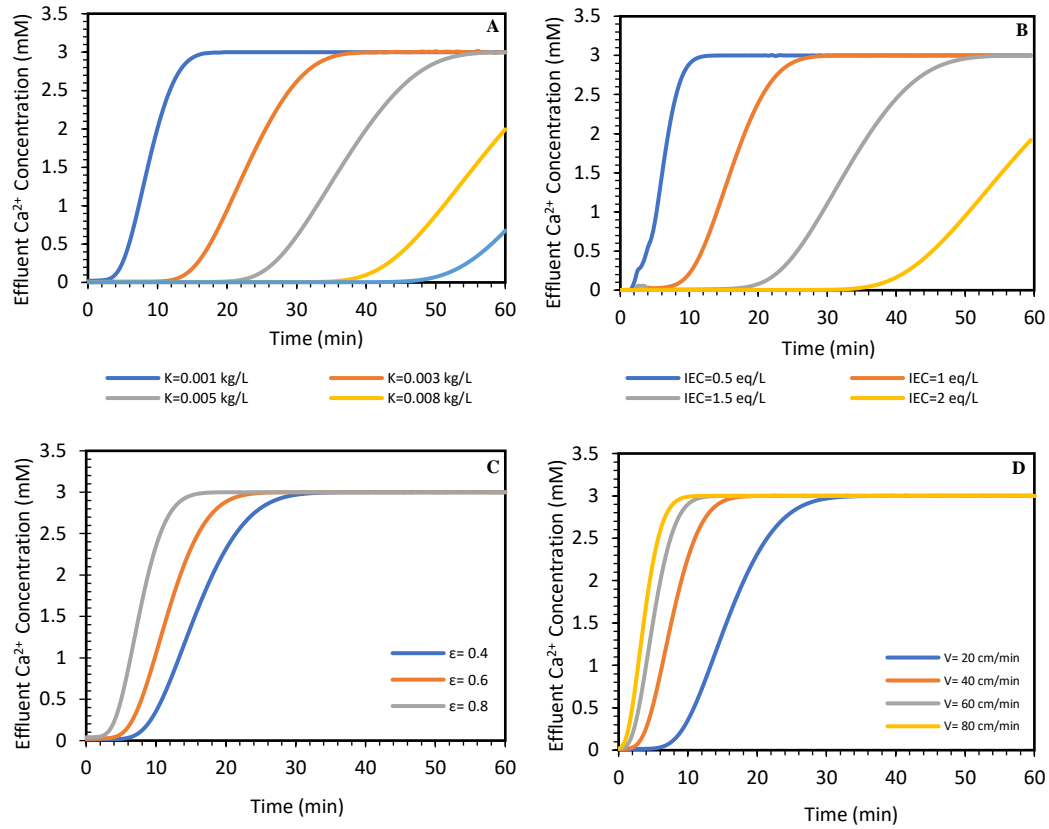


Figure 3.7: Effect of variation in model parameter values on breakthrough profile: (A) selectivity coefficient ( $K_{Ca/NH_4}$ ); (B) ion exchange capacity (IEC); (C) porosity ( $\epsilon$ ); (D) flow velocity ( $V$ ).

The breakthrough curve of  $Ca^{2+}$  was investigated using various  $\epsilon$  and  $V$  values ranging from 0.4-0.8 and 20-80 cm/min, respectively. Additional parameters used in the model are represented in Section 2.3, Table 2.4. The results in Figure 3.7 (C) depict an increase in  $Ca^{2+}$  uptake with a decrease in  $\epsilon$ . A decrease in  $\epsilon$  has a significant effect on the shape of the breakthrough curve. Any change applied to  $\epsilon$  results in a shift in the obtained values for breakthrough time. The results in Figure 3.7 (D) show an increase in  $Ca^{2+}$  uptake with a decrease in  $V$ . This is represented through the following breakthrough points at 6.0, 2.5, 1.0, and 0.5 minutes with an increase in  $V$ . The breakpoint is represented at the point

where the effluent  $\text{Ca}^{2+}$  concentration becomes 10% of the influent. Results from the breakthrough points show that the time needed to reach breakpoint generally occurred faster with a higher  $V$ . Also, it was observed that the values of  $V > 40$  cm/min had an insignificant effect on the shape of the breakthrough curve. Moreover, to examine the effect of  $V$  on the volume of the treated solution, the cross-sectional area ( $A$ ) of the column is assumed to be  $10\,000\text{ cm}^2$ . The  $A$  of the column is uniform signifying that  $V$  through the column bed is directly proportional to the overall volumetric flow rate ( $Q$ ) through the column bed ( $V = \frac{Q}{A}$ ). The volume of solution treated until the breakpoint is 1200, 1000, 600, and 400 L for an increase in  $V$ . An increase in  $V$  was shown to reduce the amount of water treated by the column efficiently. This is due to the decrease in contact time between  $\text{Ca}^{2+}$  and SAC exchange resins at higher  $V$ .

## 4. Conclusions

### 4.1. Determination of IEC and $K_{\text{Ca}/\text{NH}_4}$ , $K_{\text{Ca}/\text{Na}}$ , and $K_{\text{Na}/\text{NH}_4}$ by linearization

In this study, a linear system was developed for plotting experimental data leading to the determination of IEC and  $K$  values for the binary systems: Ca-NH<sub>4</sub>; Ca-Na; and Na-NH<sub>4</sub>. Two linear systems were developed to investigate IEC and  $K$ . A stability analysis was performed, and results showed that Method 2 was more stable in determining  $K$  over Method 1. The determined IEC values using linearization Method 2 for the binary system Ca-NH<sub>4</sub> are 2.26, 1.92, and 2.01 eq/L for Resins A-C, respectively. In addition, the determined IEC for binary systems Ca-Na and Na-NH<sub>4</sub> are 2.06, 2.08, and 2.03 eq/L for Resins A-C, respectively. The IEC values for Resins A and C are in good agreement with

the obtained manufacturer values. The  $K_{Ca/NH_4}$  and  $K_{Ca/Na}$  values were determined using linearization Method 2. Results showed that the determined  $K_{Ca/NH_4}$  values are 2.82, 2.87, and 3.54 kg/L for Resins A-C, respectively. In addition, the  $K_{Ca/Na}$  values are 1.55, 1.41, and 1.61 kg/L for Resins A-C, respectively. Lastly, the  $K_{Na/NH_4}$  values are 1.09, 1.08 and, 1.10 for Resins A-C, respectively. It was determined using Method 2 that SAC exchange resins initially saturated with  $NH_4^+$  were more selective towards  $Ca^{2+}$  than SAC resins saturated with  $Na^+$ . The ionic valence and hydrated radius were observed to have a strong influence over the selectivity of the resin for ions. A higher valency and a smaller hydrated radius resulted in an increased affinity of the resin for ions. In determining IEC and K, results can be used when considering column design and operation.

#### **4.2. Heavy metal removal**

The maximum percent removal of SAC exchange resins was evaluated measuring the extent of ion exchange of various heavy metals in an aqueous solution. It was confirmed that SAC exchange resins can effectively remove toxic heavy metals from a solution at a relatively low concentration of 0.1 mg/L. In a solution containing a high molar concentration of  $Ca^{2+}$ ,  $Na^+$ , and  $NH_4^+$ , SAC exchange resins were responsible for ~ 95-99% removal of toxic heavy metal ions,  $Cr^{3+}$ ,  $Pb^{2+}$ ,  $Ba^{2+}$ , and  $Cd^{2+}$ . Results suggest the use of SAC exchange resins as a pretreatment method for the removal of toxic heavy metals. Additional findings include the low percent removal of  $Hg^{2+}$  (~ 7%) and  $Ag^+$  (~ 17%) attributed to the presence of  $Cl^-$  in solution as both metal cations form insoluble precipitates with  $Cl^-$ . Anionic heavy metals,  $As^{3-}$  and  $Se^{2-}$  were observed to not be removed using SAC



exchange resins. This trend is due to the matrix of SAC exchange resins which contain a negatively charged sulfonate group that is permanently fixed to the resin, therefore, giving a negatively charged matrix.

### **4.3. One-dimensional column model**

A mathematical model has been used to predict the performance of a SAC exchange resin column for the removal of  $\text{Ca}^{2+}$  from an aqueous solution. Results showed that the use of SAC exchange resins was an efficient method in the removal of  $\text{Ca}^{2+}$ . A sensitivity analysis performed on the mathematical model parameters showed that the variation in  $K$  and IEC greatly influenced the breakthrough time as an increase in both parameters resulted in greater  $\text{Ca}^{2+}$  uptake. Additional observations included an increase in  $\text{Ca}^{2+}$  uptake with a decrease in  $\epsilon$  and  $V$ . Modelling results can be used to optimize the design of ion exchange systems for the pretreatment of inorganic cations which can reduce membrane scaling.

### **4.4. Future Work**

#### **4.4.1. Determination of IEC and $K$ of multicomponent systems**

In this study, a linear system was developed for plotting binary experimental data leading to the determination of IEC and  $K$ . Since this study only focused on the determination of IEC and  $K$  of binary systems, future work should focus on expanding the linear system to accommodate multicomponent systems. To predict multicomponent equilibrium data, binary equilibrium data can be combined. Detailed knowledge of

multicomponent equilibrium data is essential for the proper understanding and development of ion exchange column design and performance.

#### **4.4.2. One-dimensional column model**

A one-dimensional ion exchange column model was developed to simulate the removal of  $\text{Ca}^{2+}$  from a feed solution containing  $\text{Ca}^{2+}$  and  $\text{NH}_4^+$ . A limitation within the developed column model is the inability to achieve high  $K_{\text{Ca}/\text{NH}_4}$  values. Therefore, future studies should focus on possible model modifications to achieve high  $K_{\text{Ca}/\text{NH}_4}$ . In addition, an assumption of instantaneous equilibrium made within model development allows for a potential overestimation of  $\text{Ca}^{2+}$  uptake. Future model development should focus on the addition of diffusivity coefficients with the use of the Nernst-Haskell equation. Lastly, future model simulations should focus on the removal of inorganic cations that contribute to membrane scaling. The addition of such inorganic ions into the model will allow for the pretreatment of various wastewater solutions before the use in membrane processes.

## References

- Abo-Fartha, S.A., Abdel-Aal, A.Y., Ashour, I.A., Garamon, S.E. (2009). Removal of some heavy metal cations by synthetic resin purolite C100. *Journal of Hazardous Materials*, 169, 190-194.
- Alyüz, B., & Veli, S. (2009). Kinetics and equilibrium studies for the removal of nickel and zinc from aqueous solutions by ion exchange resins. *Journal of Hazardous Materials*, 167, 482-488.
- Akpor, O.B., Ohiobor, G.O., Olaolu, T.D. (2014). Heavy metal pollutants in wastewater effluents: Source effects and remediation. *Advances in Bioscience and Bioengineering*, 2(4), 37-43.
- Ayoub, G.M., Acra, A., El Fadel, M., Koopman, B. (2001). Heavy metal removal by coagulation with seawater liquid bittern. *Journal of Environmental Engineering*, 127(3), 196-202.
- Bauman, W., & Eichhorn, J.J. (1947). Fundamental Properties of Synthetic Cation Exchange Resins. *American Chemical Society*, 69, 2830.
- Benjamin, M.M., & Lawler, D.F. (2013). *Water Quality Engineering: Physical/ Chemical Treatment Processes*. John Willey & Sons Inc.
- Bieber, H., Steidler, F.E., & Selke, W.A. (1954). *Chemical Engineering Progress Symposium Series, No.14*, 50, 17-21.
- Bose, P., Bose, M.A., Kumar, S. (2002). Critical evaluation of treatment strategies involving adsorption and chelation for wastewater containing copper, zinc, and cyanide. *Advances in Water Treatment and Pollution Prevention*, 7, 179-195.
- Boyd, G., Adamson, A.J., Myers Jr., L.S. (1947). The Exchange Adsorption of Ions from Aqueous Solutions by Organic Zeolites. II. Kinetics. *American Chemical Society*, 69(11), 2836-2848.
- Boyer, W.D.A. (1997). *Determination of Ion Exchange Parameters for Binary Systems and Application to Ternary Systems*. [Master's Thesis, McMaster University].
- Boyer, W.D.A., Baird, M.H.I and Nirdosh, I. (1999) Ion Exchange Equilibria in Binary and Ternary Systems. *The Canadian Journal of Chemical Engineering*, 77, 92-98.
- Bochenek, R., Sitarz, R., Antos, D. (2011). Design of continuous ion exchange process for the wastewater treatment. *Chemical Engineering Science*, 66, 6209-6219.

- Brewster, E. T., Ward, A. J., Mehta, C. M., Radjenovic, J., & Batstone, D. J. (2017). Predicting scale formation during electro dialytic nutrient recovery. *Water research*, 110, 202-210.
- Canadian Council of Ministers of the Environment (2006). Review of the State of Knowledge of Municipal Effluent Science and Research. [https://www.ccme.ca/files/Resources/municipal\\_wastewater\\_effluent/pn\\_1424\\_mwe\\_md1\\_bylaw\\_dvlpmt\\_rpt.pdf](https://www.ccme.ca/files/Resources/municipal_wastewater_effluent/pn_1424_mwe_md1_bylaw_dvlpmt_rpt.pdf)
- Canadian Council of Ministers of the Environment (2009). Model Sewer Use Bylaw Limit. [https://www.ccme.ca/files/Resources/municipal\\_wastewater\\_effluent/pn\\_1421\\_model\\_sewer\\_use\\_bylaw\\_guidance\\_doc\\_e.pdf](https://www.ccme.ca/files/Resources/municipal_wastewater_effluent/pn_1421_model_sewer_use_bylaw_guidance_doc_e.pdf)
- Chartrand, Z.G. (2018). *The Selective Ion- Exchange Removal of Ammonia from Mining Wastewater*. [Master's Thesis, University of Ottawa]. Semantic Scholar.
- Crank, J., Park, G. (1968). *"Diffusion in Polymers"*. Academic Press.
- Crittenden, J.C., Rhodes, R. R., Hand, D.W., Howe, K.J., and Tchobanoglous, G. (2012). *MWH's Water Treatment: Principles and Design, Third Edition*. John Wiley & Sons, Inc.
- Donnan, F.G. (1924). The Theory of Membrane Equilibria. *American Chemical Society*, 1(1), 73-90.
- Dranoff., J., & Lapidus, L. (1957). Equilibrium in Ternary Ion Exchange Systems. *Industrial and Engineering Chemistry*, 49(8).
- DuPont (2019, November). DuPont Ion Exchange Resins: Proper Storage Conditions for DuPont Ion Exchange Resins. <https://www.dupont.com/content/dam/dupont/amer/us/en/watersolutions/public/documents/en/45-D01093-en.pdf>
- Environment and Climate Change Canada (ECCC). (2012). Heavy Metals. <https://www.ec.gc.ca/air/default.asp?lang=En&n=69E279CF-1&wbdisable=true>
- Fievet, P. (2015) Donnan Potential. In: Encyclopedia of Membranes. Springer.
- Foster, J.T.T., Hu, Y., & Boyer, T.H. (2017). Affinity of potassium-form cation exchange resin for alkaline earth and transition metals. *Separation and Purification Technology*, 127, 229-237.

- Gaines G.L., & Thomas H.C. (1953). Adsorption studies on clay materials. II. A formulation of the thermodynamics of exchange adsorption, *The Journal of Chemical Physics*, 21 (4), 714-718
- Greenlee, L.F., Lawler, D.F., Freeman, B.D., Marrot, B., Moulin, P. (2009). Reverse osmosis desalination: water sources, technology, and today's challenges. *Water Research*, 43(9), 2317-2348.
- Harland, C.E. (1994). *Ion Exchange: Theory and Practice*. Royal Society of Chemistry.
- Helfferich, F. G. (1962). *Ion Exchange*. Dover Publication Inc.
- Hubicki, Z., & Kolodynska, D. (2012). Selective Removal of Heavy Metal Ions from Waters and Waste Wasters Using Ion Exchange Methods. *Intech*. <http://dx.doi.org/10.5772/51040>
- Jackson, M.B., & Bolto, B.A. (1990). Effect of Ion-exchange resin structure on nitrate selectivity. *Reactive Polymers*, 12, 277-290.
- Jüttner, K., Galla, U., Schmieder, H. (2000). Electrochemical approaches to environmental problems in the process industry. *Electrochimica Acta*, 45(15-16), 2575-2594.
- Klein G.D., Tondeur D. and Vermeulen T. (1967). Multicomponent ion exchange in fixed beds. *Industrial and Engineering Chemistry Research*, 6(3), 339-351.
- Kressman, T.R.E., & Kitchener, J.A. (1949). Cation Exchnage with a synthetic phenolsulfonate resin. *Journal of Chemical Society*, 1208.
- Kurniawan, T.A., Chan, G.Y.S., Lo, W., Babel, S. (2006). Physico–chemical treatment techniques for wastewater laden with heavy metals. *Chemical Engineering Journal*, 118, 83-98.
- Lenntech Water Treatment Solutions (2018, May). Amberlite™ IRC120 NA Ion Exchange Resin. <https://www.lenntech.com/Data-sheets/DOW-177-03802-IRC120-Na-L.pdf>
- Manning, M.J. & Melsheimer, S.S. (1983). Binary and Ternary Ion Exchange Equilibria with a Perfluorosulfonic Acid Membrane. *Industrial and Engineering Chemistry*, 22, 311-317.
- Marinsky, J.A. (1967). Predication of Ion-Exchange Selectivity. *Journal of Physical Chemistry*, 76(6), 1572-1578.
- Mehablia M.A., Shallcross D.C. and Stevens G.W. (1994). Prediction of multicomponent

- ion exchange equilibria. *Chemical Engineering Science*, 49(14), 277-2286.
- Mikhaylin, S., & Bazinet, L. (2016). Fouling on ion-exchange membranes: Classification, characterization and strategies of prevention and control. *Advances in colloid and interface science*, 229, 34-56.
- Mitsubishi Chemical. (2019). Ion Exchange Resins: Gel type Diaion™ SK Series. [https://www.diaion.com/en/products/ion\\_exchange\\_resins/strongly\\_acidic\\_cation/index.html](https://www.diaion.com/en/products/ion_exchange_resins/strongly_acidic_cation/index.html)
- Mondor, M., Ippersiel, D., Lamarche, F., and Masse, L. (2009). Fouling characterization of electro dialysis membranes used for the recovery and concentration of ammonia from swine manure. *Bioresource. Technology*, 100(2), 566–571.
- Nachod F.C. (1949), *Ion Exchange, Theory and Application*. Academic Press Inc.
- Nightingale, E.R. (1959). Phenomenological theory of ions salvation: effective radii of hydrated ions. *The Journal of Physical Chemistry*, 63,1381-1387.
- Oancea, M.S., Drinkal, C., & Höll, W.H. (2008). Evaluation of exchange equilibria on strongly acidic ion exchangers with gel-type, macroporous and macronet structure. *Reactive & Functional Polymers*, 68, 492-506.
- Patel, H. (2019). Fixed bed column adsorption study: a comprehensive review. *Applied Water Science*, 9(45).
- Phipps, A.M., & Hume, D.N. (1967). Ion exchange processes in liquid ammonia. *Analytical Chemistry*, 39(14), 1755-1762.
- Pieroni L. and Dranoff J. (1963). Ion exchange equilibria in a ternary system. *AIChE Journal*, 9(1), 42-45.
- Potts, D.E., Ahlert, R.C., Wang, S.S. (1981). A critical review of fouling of reverse osmosis membranes. *Desalination*, 36, 235-264.
- Prajapati, S. (2014). *Cation Exchange for Ammonia Removal from Wastewater*. [Master's Thesis, Tampere University of Technology].
- Purolite. (2018). Product Information Shallow Shell™ SSTC60 Resin for Softening. [https://www.purolite.com/dam/jcr:93bd98dd-de72-47a4-b6783f31f03ae318/SST60%20Engineering%20Bulletin%20\\_2018FINAL.pdf](https://www.purolite.com/dam/jcr:93bd98dd-de72-47a4-b6783f31f03ae318/SST60%20Engineering%20Bulletin%20_2018FINAL.pdf)
- Rengarji, S., Joo, C.K., Kim, Y.H., Yi, J.H. (2003). Kinetics of removal of chromium from water and electronic process wastewater by ion exchange resins: 1200H, 1500H, and IRN97H. *Journal of Hazardous Material*, 102 (2-3), 257-275.

- Rengarji, S., Yeon, K.H., & Moon, S.H. (2001). Removal of chromium from water and wastewater by ion exchange resins. *Journal of Hazardous Material*, 87(1-3), 278-287.
- Saidi, M (2010). Experimental studies on effect of heavy metals presence in industrial wastewater on biological treatment. *International Journal of Environmental Sciences*, 1(4), 666-676.
- Sahu, P., Jaiswani, R. (2018). Ion Exchange Resins: An approach for the Development of Advanced Materials with Industrial, Pharmaceutical and Clinical Applications. *International Journal of Advance research, Ideas and Innovations in Technology*, 4(1).
- Sapari, N., Idris, A., Hisham, N. (1996). Total removal of heavy metal from mixed plating rinse wastewater. *Desalination*, 106, 419-422.
- Shallcross, D.C., Herrmann, C.C., McCoy, B.J. (1988). An improved model for the prediction of multicomponent ion exchange equilibria. *Chemical Engineering Science*, 43(2), 279-288.
- Smith R.P., & Woodburn E.T. (1978). Prediction of multicomponent ion exchange equilibria for ternary system  $\text{SO}_4^{2-}-\text{NO}_3^--\text{Cl}^-$  from data of binary systems, *AIChE Journal*, 24(4), 577-587.
- Soldano, B.A., Larson, Q.V., & Myers, G.E.J. (1955). *American Chemical Society*, 77.
- Spiro, A.D. (2009). Ion- Exchange Resins: A Retrospective from Industrial and Engineering Chemistry Research. *American Chemical Society*, 488, 388-398.
- Taty-Costodes, V.C., Fauduet, H., Porte, C., Ho, Y. (2005). Removal of lead (II) ions from synthetic and real effluents using immobilized *Pinus sylvestris* sawdust: Adsorption on a fixed-bed column. *Journal of Hazardous Materials*, 123 (1-3), 135-144.
- Tombalakian, A., Yeh, C.Y., & Graydon, W.F.J. (1967). *Journal of Physical Chemistry*, 71, 435.
- Tyła, M. (2019). Assessment of Heavy Metal Pollution and Potential Ecological Risk in Sewage Sludge from Municipal Wastewater Treatment Plant Located in the Most Industrialized Region in Poland—Case Study. *International Journal of Environmental Research and Public Health*.

- Vasquez G., Arce A., Mendez R., & Blasquez R. (1986). Ion-exchange equilibria: study of the Na<sup>+</sup> Mn<sup>2+</sup>, Na<sup>+</sup>, Ni<sup>2+</sup> and Na<sup>+</sup>, Cu<sup>2+</sup> exchanges on several Lewatit cation exchangers. *The Journal of Chemical Engineering Data*, 31(4), 466-469.
- Wachinski, A. M. (2006). *Ion exchange treatment for water*. American Water Works Association.
- Wheaton R.M., Lefevre. (2000). DOWEX Ion Exchange Resins: Fundamentals of Ion Exchange. <https://www.lenntech.com/Data-sheets/Dowex-Ion-Exchange-Resins-Fundamentals-L.pdf>
- Wilson, G. M. (1964). Vapor-liquid equilibrium XI. A new expression for the excess energy of mixing. *Journal of the American Chemical Society*, 86, 127-130.
- Yang, X.J., Fane, A.G., MacNaughton.S. (2001). Removal and recovery of heavy metals from wastewater by supported liquid membranes. *Water Science Technology*, 43(2), 341–348.
- Yu, Z., Qi, T., Qu., J., Wang, L., Chu, J. (2009). Removal of Ca (II) and Mg (II) from potassium chromate solution on Amberlite IRC 748 synthetic resin by ion exchange. *Journal of Hazardous Materials*, 167, 406-412.
- Zagorodni, A. A. (2007). *Ion Exchange Materials: Properties and Applications*. Elsevier.